Bioresources and Bioprocessing

RESEARCH

Open Access

Oil palm residue-based cellulose acetate membranes enhanced with zinc oxide and n-methyl pyrrolidinone for batik wastewater treatment

Belladini Lovely[1], Hasna Amalia Fauziyyah[2], Shendy Krisdayanti[2], Muhamad Zakky Irsyada[2], Lisna Efiyanti[1], Wara Dyah Pita Rengga[2], Novitri Hastuti[1,5*], R. A. Ilyas[3,4,5*], Mohd Nor Faiz Norrrahim[6*] and Victor Feizal Knight[6]

Abstract

As the world's top producers of oil palm (*Elaeis guineensis*), Indonesia and Malaysia are urged to propose a value-added valorization of its lignocellulosic biomass, oil palm empty fruit bunches (OPEFB). Meanwhile, the nations' signature 'batik' textile industries are in dire need of optimum remediation treatments of their wastewater high in harmful dyes and chemicals. Organic–inorganic hybrid systems of mixed matrix membranes (MMMs) for heavy metals removal were prepared using OPEFB-based cellulose acetate (CA) and zinc oxide (ZnO; 0.5, 0.75, 1%, w/v) in N-methyl pyrrolidinone (NMP; 89, 90, 91%, v/v). The high crystallinity (62.42%) and fibrils' web-like structure of OPEFB-CA were confirmed. Microscopic observation of OPEFB CA-NMP-ZnO membranes evidenced the porous yet smooth surface due to the use of plasticizing NMP, as well as uniform dispersion of ZnO particles. MMM 2 (0.75%ZnO; 90%NMP) was the best-performing membrane mechanically with excellent tensile strength (1.78 MPa), Young's modulus (0.13 GPa), and elongation-at-break (2.59%), while thermal stability ($T_{d,5\%}$, 291 °C) improvement was also highlighted. Pores characteristics on size, volume, and surface area were discussed, too. Remediation performance was excellent even at high (20%) effluent concentration reaching 28% and 65% removal of Cu and Pb, respectively, by MMM 1 (0.5%ZnO; 89%NMP). These findings confirmed the promising prospect of the developed membranes as a wastewater remediation treatment, including in textile industries.

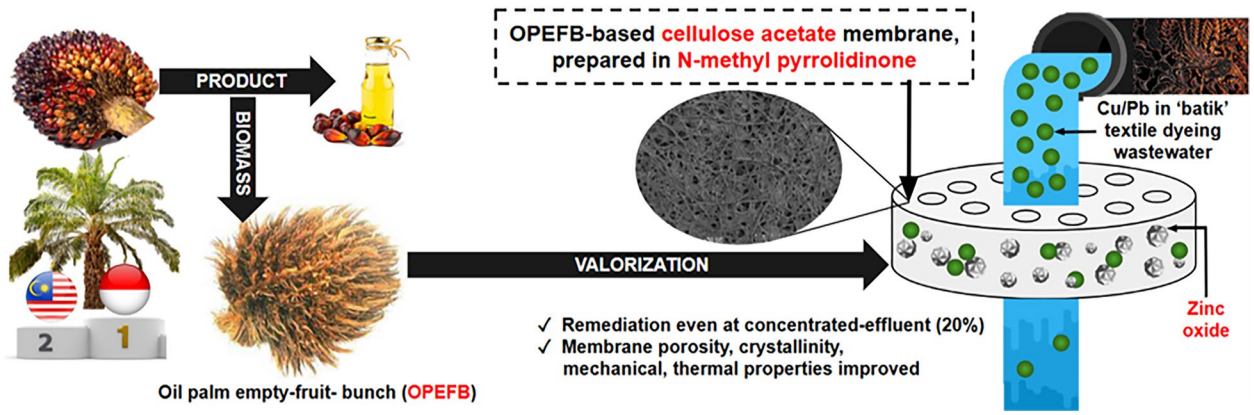
Keywords Oil palm empty fruit bunch (OPEFB), Membrane, Cellulose acetate, Zinc oxide (ZnO), N-methyl pyrrolidinone (NMP), Remediation

*Correspondence:
Novitri Hastuti
novi043@brin.go.id; novitri.forester@gmail.com
R. A. Ilyas
ahmadilyas@utm.my
Mohd Nor Faiz Norrrahim
faiz@upnm.edu.my
Full list of author information is available at the end of the article

Springer Open

© The Author(s) 2025. **Open Access** This article is licensed under a Creative Commons Attribution 4.0 International License, which permits use, sharing, adaptation, distribution and reproduction in any medium or format, as long as you give appropriate credit to the original author(s) and the source, provide a link to the Creative Commons licence, and indicate if changes were made. The images or other third party material in this article are included in the article's Creative Commons licence, unless indicated otherwise in a credit line to the material. If material is not included in the article's Creative Commons licence and your intended use is not permitted by statutory regulation or exceeds the permitted use, you will need to obtain permission directly from the copyright holder. To view a copy of this licence, visit http://creativecommons.org/licenses/by/4.0/.

Graphical Abstract



Introduction

'Batik' textile dyeing technique originates from the Indonesian-Javanese and can be traced back to the seventeenth century and is a UNESCO-recognized heritage of Southeast Asia's Malay nations. 'Batik' applies melted wax and resin dye-based intricate designs on a cloth prior to multiple washing and boiling. The generated effluent is typically in large amounts and highly polluted yet handled through minimum to no proper wastewater treatment, risking the environment (Zakaria et al. 2023; Ramakreshnan et al. 2020; Buthiyappan et al. 2016; Rezagama et al. 2020). Even generally, textiles are among the world's highest effluent-generating sectors (Javed et al. 2025; Slama et al. 2021; Jorge et al. 2023). Though authentic 'batik' productions use plant or insect-based dyes, the large-scale demands forced the substitution to the use of various types of synthetic dyes (Slama et al. 2021; Ghaly et al. 2013; Mani et al. 2019; Rashidi et al. 2012). In consequence, the environmental concern possessed by the resulting wastewater is often of significance due to the posed pollutants, not only the excess wax, chemicals, grease, surfactant, silicate, soluble salts, odor, and color, but also suspended/dissolved solids, biochemical oxygen demand (BOD), chemical oxygen demand (COD), and trace heavy metals (e.g., Cu, Pb, Cr, Co, Ni, As, Cd, Zn, Hg). Dyes' complex molecular structures enable the pollutants to remain in the water for a prolonged time, disrupting the sunlight penetration depth necessary for photosynthesis and re-oxygenation of the existing aquatic, photoautotrophic organisms. Subsequently, the water's dissolved oxygen (DO) concentration is reduced while BOD rises (Budiyanto et al. 2018; Azha and Ismail 2021; Juliani 2021; Rahmaniah et al. 2019; Lestari et al. 2019; Masupha 2008; Odubanjo et al. 2021; Desa et al. 2019).

To solve such a recurring issue, membrane technology is among the most applied heavy metal removal approaches, including wastewater treatment. Membranes porosity, selectivity, and permeability filter and separate substances by size using pressure when wastewater is pumped through modules. This approach is low-energy and easily operable with minimum to no pollution (Z.-P. Wang et al. 2011; Istirokhatun et al. 2021). According to the retained substances' particle size, membrane separation can be classified into reverse osmosis, nanofiltration, ultrafiltration, and microfiltration, from the biggest to smallest pore diameter, ranging from 100 nm–10 µm to 0.1–1 nm (Z. Yang et al. 2019). However, these technologies face some prevalent constraints, including the accumulated dissolved solids and dyes when treating complex and highly concentrated effluents, including those of textile dyeing industries. Fouling requires indispensable, sometimes multiple, pre/post-treatments (C.-Z. Liang et al. 2014; Alventosa-deLara et al. 2014; Amin and Nizam 2016). Thus, membrane modifications have been extensively studied to overcome this main limitation, one of which is the introduction of organic–inorganic hybrid membranes (or mixed matrix membranes; MMMs). MMMs combine organic polymer (as the matrix or continuous phase) with inorganic porous ceramics (as the filler or dispersed phase). As one of MMMs' commonly used inorganic materials, metal oxides are carbon-based and advantageous due to their chemical, mechanical, and thermal stabilities owing to the uniform macroporous support and meso-/micro-porous barrier layer structure. Their charge transport and specific electronic structure arrangements give them a high adsorption

capacity (Jebelli et al. 2024). Metal oxide-driven photocatalysis generates oxidizing species during photon irradiation on the surface of a semiconducting material, which decomposes organic pollutants in wastewater within a short time, is scalable and cost-effective, without persistent by-products (Abdelsamad et al. 2018; Karthik et al. 2024; Shukla et al. 2025; Etafo et al. 2024). Combining these features with polymers is proven to be among the alternatives to intensify the permeability and selectivity, surpassing aging trade-offs empirically observed for the neat-polymeric membranes (Z. Yang et al. 2019; Kamble et al. 2021; Nuhnen and Janiak 2021; Vasanth and Prasad 2019; Tanvidkar et al. 2023).

In selecting polymeric ingredients for MMMs, cellulose is the Earth's most abundant polymer, naturally biodegradable and extractable from wood, plants, algae, bacteria, and tunicate. Cellulose is easy to modify and compatible, hence its multifaceted applicability, including incorporation with organic/inorganic materials in a hybrid system (Jebelli et al. 2024; Abdelsamad et al. 2018; Karthik et al. 2024). Cellulose acetate (CA), a cellulose ester derivative, is of particular interest to membrane researchers, as evidenced by the spike of interest in the past decade (Vatanpour et al. 2022; Islam et al. 2023). CA excels in its ease of availability, low price, biodegradability, low/non-toxicity, hydrophilicity, chemical–mechanical–thermal stability, water affinity, film-formability, desalting ability, transport properties, design versatility, facile manufacturing, and environmental benignity (Miao et al. 2020; Wei et al. 2020; Fischer et al. 2008; Zugenmaier 2004; Sharma et al. 2012; Syamani 2020; Tahazadeh et al. 2021; Rajeswari et al. 2017; Ghaee et al. 2016; Rana et al. 2022; Febriasari et al. 2024; Jamaluddin et al. 2022). However, pristine CAs suffer from a few vital disadvantages, such as inert functional groups, poor chemical–thermal–mechanical stability, and incompatibility with affinity-based adsorption separation. Compared to hydrophobic membranes, neat-CA membranes provide a slower solvent/coagulant diffusion capacity during phase inversion preparation. This leads to the membrane's dense skin layer, hence the low porosity, flux, and protein rejection ratio. Pure-CA membranes also operate at a narrow range of pH and temperature (Sivakumar et al. 1999; Zavastin et al. 2010; Arthanareeswaran and Thanikaivelan 2010; Karthik et al. 2024) and are less resistant to microbial corrosion, oxidation, and other organic pollutants (Shenvi et al. 2014; Zhou et al. 2016). Addressing this gap, combining metal oxides and CA in a MMMs system provides antifouling, anti-bacterial/fungal, photocatalytic, and UV-blocking features. Cellulose-based material surfaces act as ideal carriers after their hydrophilic substrates to accelerate nucleation and growth of metal oxide particles onto them. Compared with other popularly reported inorganic additives for membranes (e.g., titanium dioxide (TiO_2), alumina (Al_2O_3)), zinc oxide (ZnO) is superior for cost-effectiveness, low toxicity, and specific surfaces owing to its crystallographic structure (S. Liang et al. 2012; Tam et al. 2008; Alhalili et al. 2021; Hong and He 2014; Asiri et al. 2021; Rashid et al. 2022). ZnO excelled in heavy metal ion removal rate when compared with other alternatives (i.e., a commercial TiO_2 P25 and a modified version) (Hua et al. 2012; Lee et al. 2005). A low-temperature, low-cost dye removal study also proved ZnO's unique nano-rod/tube shapes' influence in superior photocatalytic properties against TiO_2 and ZnO-TiO_2 combination (Guo et al. 2011; Sheikh et al. 2020). The reported improvements on ZnO-incorporated membranes include permeation, flexibility, hardness, dye degradation capacity, hydrophilicity, surface roughness, profile valley depth, mechanical, thermal, and chemical stability (Tang et al. 2006; Rajeswari et al. 2017; Alhalili et al. 2021; Asiri et al. 2021; Mahlangu et al. 2017). The essential strong hydrophilicity can be retained by adhering to the hydrophilic functional groups (e.g., –OH, $–SO_3H$, –COOH) on top of the chemical bonding between oxide and the pairing polymer (Wu and Xue 2011; Shen et al. 2012, 2020). The promoted hydrophilicity may contribute to fouling mitigation as most foulants are hydrophobic (Vatanpour et al. 2022). The concern regarding ZnO's toxicity has been debunked as well (Balta et al. 2012; Franklin et al. 2007; Ngulube et al. 2024), confirming its safety. Especially by incorporating ZnO in a carrier (CA), potential leaching could be kept below the standard levels for effluent reuse and discharge, proving its long-term stability (Zhang et al. 2019; Ben Dassi et al. 2021).

The solvent used to prepare CA-based membranes also matters. Compared to other popular contenders (e.g., acetone, dimethylformamide (DMF), or dimethylacetamide (DMAc), tetrahydrofuran (THF)), N-methyl pyrrolidinone (NMP) possesses a myriad of prospects. These include dispersibility, permeate concentration, water flux, sorption selectivity, tensile strength, elastic modulus, transparency, roughness, tailorable porosity, as well as post-use nodule/void sizes/shapes and surface morphology. NMP's volatility or vapor pressure was evidenced to improve CA chains relaxation and membrane formability, with the plasticization effect via the increased free volume of CA chains. NMP's desired boiling point also highly influences thermal stability (Tabe-Mohammadi et al. 2001; van den Berg et al. 2007; Cindradewi et al. 2021; Lee et al. 2018). The potentials of CA-acetone-ZnO (Rajeswari et al. 2017; El-Noss et al. 2020; Durthi and Rajulapati 2018; Hassan et al. 2017), CA-DMF-ZnO (Asiri et al. 2021; Alhalili et al. 2021; M. Ali et al. 2011; Chaurasia et al. 2010; H. S. Hassan et al.

2017), CA-DMAc-ZnO (Hassan et al. 2017; Zhou et al. 2023; Nasouri 2019; Suwantong and Supaphol 2015), and CA-THF-ZnO (Douna et al. 2023) systems have been studied; however, CA-NMP-ZnO has yet to be explored to date especially for wastewater remediation, implying its novelty.

Speaking of the cellulosic source in preparing CA, agricultural wastes have become among the most extensively studied renewable options. Cultivated mainly for crude palm oil, oil palm (*Elaeis guineensis*) is a tropical-perennial oleaginous crop that grows along equatorial Southeast Asia, South America, and Africa (Wahid et al. 2005; Corley and Tinker 2008). Despite originating from West/Central Africa (Mutsaers 2019), Indonesia, Malaysia, and Thailand are named as today's top producers, where 2024 global production surpassed 80 million MT (United States Department of Agriculture 2024). Oil palm has exceptional productivity (36% of global oils while taking merely 8% of the oil croplands), yield (13, 8, and 7 times greater than soybean, sunflower, and rapeseed, respectively), and economic life span (25 years) (Ritchie et al. 2023; Chang 2014; Tye et al. 2011). In line with such unprecedented growth, a vast quantity of waste is generated every year. Per T CPO, half of the generated solid wastes (~ 1.1–1.5 T) is a residue acquired post-sterilization and stripping of the fresh fruit bunches, called oil palm empty-fruit-bunch (OPEFB) (Dahnum et al. 2015; Dalimin 1995; Loh 2017). OPEFB is characterized by its brown color, hard/tough structure, bulk density, low calorific value, and high contents of moisture (> 60% of total weight), ash, and mineral matter, ultimately leading to its low conversion efficiencies and economic value (Sulaiman et al. 2010; Ahmad et al. 2019; Hassan et al. 2010; Chang 2014). OPEFB utilization has been limited to low-value-added applications such as mulch, fertilizer/compost, manure, and cultivation substrate, whereas direct burning may cause incomplete combustion and the release of fine ash or white smoke, or even worse, fouling and pest attraction when left unattended; displaying a serious disposal challenge (Geng 2013; Kerdsuwan and Laohalidanond 2011; Yusoff 2006; Law et al. 2007). Fortunately, OPEFB holds vast potential as it contains an exceptionally high amount of cellulose (40–65%) while not disrupting the security of lignocellulosic sources intended for food (corn, soybean, coconut) or forest/plantation (wood, cotton) (Hornung 2014; Yusoff 2006; Abdullah and Sulaiman 2013; Razali et al. 2017). OPEFB-derived cellulose is also proven to be remarkably high in purity (Megashah et al. 2018). However, despite the great prospect, OPEFB utilization in cellulose acetate-based MMMs has yet to be studied. Hence, OPEFB makes as an attractive and novel cellulosic material, particularly for the development of CA-NMP-ZnO-based membranes. The use of such vastly available, underutilized, and locally sourced biomass for the nations' signature 'batik' wastewater treatment highlights this work's significance. The effect of NMP and ZnO addition was hypothesized to promote the final functional properties of CA membrane, not only the heavy metal remediation performance, but also the physical, mechanical, morphological, and thermal stability.

Materials and methods

Materials

Oil palm empty-fruit-bunch (OPEFB) was provided by a local, traditional farm in Cibadak, West Java, Indonesia. Distilled water, ethanol, glacial acetic acid (CH_3COOH), sulfuric acid (H_2SO_4, 98%, v/v), acetic anhydride ($C_4H_6O_3$), N-methyl-2-pyrrolidone or NMP (C_5H_9NO), zinc oxide (ZnO), dimethyl sulfoxide or DMSO (C_2H_6OS), sodium hydroxide (NaOH), hydrochloric acid (HCl), and phenolphthalein ($C_{20}H_{14}O_4$) were purchased from Merck & Co., Inc. (Rahway, NJ, USA). Commercial-grade cellulose was from Sigma-Aldrich (St. Louis, MO, USA).

Cellulose acetate (CA) preparation

Cellulose acetate (CA) was prepared from oil palm empty-fruit-bunch (OPEFB) dry pulp whose moisture content was tested using a MOC63u moisture analyzer (Shimadzu Corporation, Kyoto, Japan) before the extraction. The activation process was begun by dissolving OPEFB pulp (5 g) into glacial acetic acid (150 mL) before being continuously stirred (1500 rpm, 38 °C, 3 h). Next was the acetylation step by adding acetic anhydride (45 mL) and 98%-sulfuric acid (1 mL) as catalyst and back being stirred (1500 rpm, 25 °C, 2.5 h). For the hydrolysis stage, distilled water (6 mL) and glacial acetic acid (15 mL) were added to stop the acetylation, then stirred again under low heat (1500 rpm, 50 °C, 30 min). To start the sedimentation process, the mixture was centrifuged (4000 G, 25 °C, 10 min) in a 50 mL tube to separate the pellet from the supernatant. The resulting pellet was extracted using filter paper before drying in the oven (50 °C, 6 h). Identical steps were conducted using commercial cellulose to prepare commercial CA.

Membrane preparation

Cellulose acetate (CA) membrane was prepared using the synthesized CA (5%) and three different variations of added NMP and ZnO, respectively (Table 1). Firstly, CA (0.5 g) was dissolved in dimethyl sulfoxide (DMSO; 10 mL). NMP was diluted in distilled water based on the desired concentration, while ZnO was prepared in DMSO (10 mL). Afterward, the diluted NMP and ZnO were added into CA and stirred under low heat (60 °C,

Table 1 Content of different CA membrane types

OPEFB CA-NMP-ZnO membranes	NMP (%, v/v)	ZnO (%, w/v)
MMM 1	89	0.50
MMM 2	90	0.75
MMM 3	91	1

3 h). The solution was left to sit for an hour at room temperature to remove air bubbles. The membrane was prepared using a solution casting technique where the mixture was poured into a petri dish and dried (55 °C, 20 h) to let NMP (solvent) evaporate.

Crystallinity

The relative crystallinity of cellulose and CA was investigated using SmartLab (Rigaku Corporation, Wilmington, MA, USA) X-ray diffraction (XRD), which produced spectra that plot X-ray diffraction angle (2θ) vs intensity. The popularly easy and time-efficient Segal's "height XRD" method (Segal et al. 1959) was used to determine the crystallinity index (CrI), which measures the intensity ratio between the crystalline and amorphous peaks in the resulting spectra. The formula used is below, where I_{am} is the minimum intensity of the amorphous peak (or the maximum point where the entirely amorphous region is located) at around 2θ = 18°–19°, and I_{total} is the maximum intensity of the crystalline/major peak at around 2θ = 22°–23° (Nurhadi et al. 2022; Park et al. 2010).

$$CrI(\%) = 1 - \frac{I_{am}}{I_{total}}$$

Morphological and elemental analysis

The surface morphology and elemental distribution of cellulose, CA, and ZnO were characterized by the NeoScope JSM-6510LV (JEOL Ltd., Tokyo, Japan) Scanning Electron Microscope–Energy Dispersive X-ray Spectroscopy (SEM–EDS), producing SEM micrographs and EDS mapping, field-of-view images, and energy vs. intensity spectra. It was then mounted onto a pin stub mount using copper tape before being coated with gold at 20 mA. Specimens were subsequently imaged under a high vacuum at different operating voltages and magnifications: 3 kV and 50–1000× for SEM; and 15 kV and 1000× for EDS.

Porosity

The membranes' adsorption–desorption isotherms and pore characteristics (surface area, volume, and radius) were determined with a NOVA-4200e surface area and pore size analyzer (Anton Paar QuantaTec Inc., Boynton Beach, FL, USA) at degassing temperature of 120 °C (3 h) using the Brunauer–Emmett–Teller (BET) and Barrett–Joyner–Halenda (BJH) methods.

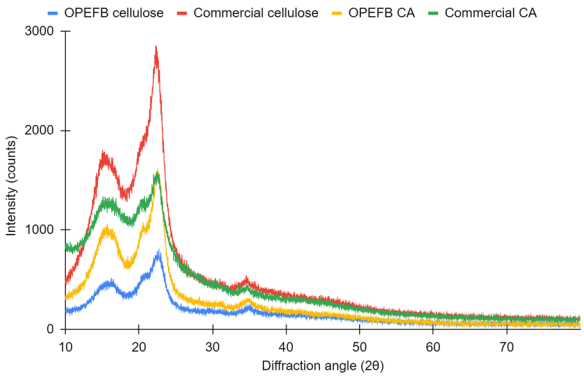


Fig. 1 XRD diffraction spectra of cellulose and CA

Mechanical properties

The mechanical testing was measured according to ASTM D638-22 (ASTM International 2022) with Universal Testing Machines (UTM) AGS-X (Shimadzu Corporation, Kyoto, Japan). The membrane's tensile strength was measured with 5 kN preload at a test speed of 5 mm/min until the films (2 × 5 cm) were ruptured and calculated from the ratio of maximum load to the cross-sectional area.

Thermal property

Thermogravimetric analysis (TGA) was performed using a Simultaneous Thermal Analyzer (STA) 6000 (PerkinElmer, Shelton, CT, USA) that plots temperature vs weight change. The sample (5–15 mg) was spread in the pan to maximize surface area. It was then ramped at 10 °C/minute between 20 and 500 °C.

Remediation performance

The concentration of heavy metals of copper (Cu) and lead (Pb) in the liquid waste was determined using a PinAAcle 500 Flame Atomic Absorption Spectrometer (AAS) (PerkinElmer, Shelton, CT, USA) at a pressure of 1 bar. The effluent of a local 'batik' factory wastewater in different concentrations (10, 15, and 20%) was employed.

Results and discussion

Crystallinity

Figure 1 presents the diffraction peaks of cellulose and CA. The crystallinity index (CrI) is measured by determining two distinct peaks: 1) the sharp, high, and obvious major or crystalline or monoclinic peak, namely I_{total} at 2θ = 20°–25°, and 2) the broad secondary or

amorphous peak, namely I_{am}, around 2θ = 12°–20°. While some minuscule peaks are likely assigned to the crystalline phase of residual salts, impurities, or trace elements, all of the arising major peaks in both OPEFB samples (cellulose and CA) could be ascribed to the characteristic patterns of the Cellulose I type. The aforesaid peaks are the Miller indices of (1$\bar{1}$0) at 2θ = 15°, (110) at 2θ = 18°, (200) at 2θ = 22.5°, and (004) at 2θ = 35° (Liu et al. 2022). This confirmed the successfully retained crystallinity profile and structure of the native cellulose contained in the rawest form as found in nature, despite the acetylation process subjected when synthesizing OPEFB CA.

CrI of all cellulose and CAs is presented in Table 2. CrI is defined as the mass ratio of the crystalline substance in the total dry sample based on the resulting XRD crystallographic two-phase model (Daicho et al. 2018). The preservation of high crystallinity was also confirmed in its CrI value of 62%. Unlike commercial CA, the effect of acetylation is apparent in its much lower CrI value of 34%. This is due to the substituting acetyl group, which eventually widened the interfibrillar distance and spaces between crystal facets and caused microfibrillar structure breakdown. (Daud and Djuned 2015; Fan et al. 2009; Kono et al. 1999; Barud et al. 2008; Filho et al. 2000). The promoted amorphous nature can be seen in the high intensity of the amorphous peak (I_{am} at 2θ = 19°) of the commercial CA spectra. This is related to the 'post-acetylation disorder's peak of CAs at 2θ = 8°, often cited as the principal characteristic of semicrystalline acetylated derivative cellulose. These phenomena are identical to other CA reports, including the OPEFB-derived ones (Daud and Djuned 2015; Djuned et al. 2014). This finding confirmed the remarkable prospect of OPEFB being utilized as a raw material in synthesizing cellulose acetate with a maintained high crystalline.

Table 2 Crystallinity index (CrI) of cellulose and CA

Sample	Amorphous peak		Crystalline peak		CrI (%)
	2θ	I_{am}	2θ	I_{total}	
OPEFB cellulose	18.11	312	22.72	794	61
Commercial cellulose	18.24	1314	22.40	2848	54
OPEFB CA	18.05	608	22.57	1618	62
Commercial CA	19.11	1028	22.76	1556	34

Morphological and elemental analysis

Figure 2 displays the surface SEM images of cellulose and CA. The sole difference between the two cellulose samples was the shorter/thicker microfibrils of commercial cellulose, possibly due to the source or extraction method. For example, cellulose extracted from sea plants and animals provides a significantly higher aspect ratio than those derived from wood and cotton (Panchal et al. 2018). OPEFB-derived cellulose itself displayed distinctive rod-like long microfibrils (Lai et al. 2021). Harsher pretreatments during cellulose extraction might lead to more intense dissolution of amorphous domains and longitudinal cutting of the microfibrils (Kalia et al. 2011). Both cellulose samples showed the appearance of numerous microfibrils, some of which are still strongly entangled and form thick bundles but with overall smooth surfaces. The smooth surface area of microfibrils was the outcome of the bleaching and delignification process that washed off hemicellulose, lignin, and other impurities from the raw OPEFB fiber (Susi et al. 2023).

In contrast, the surface of OPEFB-CA microfibrils appeared rougher, indicating the acetylation influence. The disrupted fibril–fibril hydrogen bonding as the aftermath of acetyl group introduction substituting hydroxyl group was also evidenced in the observed detachment of CA microfibrils from each other. However, a web-like structure was created, nonetheless. Unlike the CA

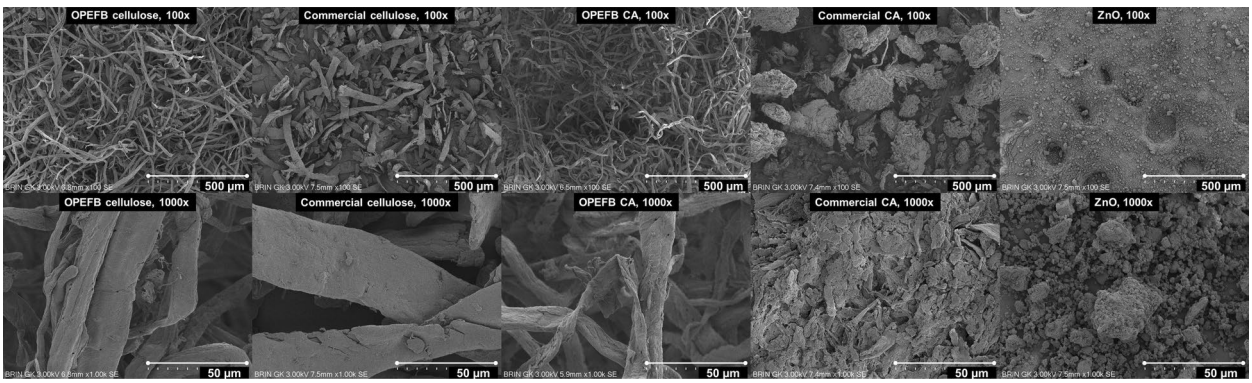


Fig. 2 SEM images of cellulose, CA, ZnO: ×100 (500 µm scale), ×1000 (50 µm scale)

prepared using the aforesaid commercial cellulose, due to the observed shorter/thicker microfibrils on top of the subjected acetylation process, commercial CA micrographs displayed phenomena of substantial agglomeration/aggregation of the microfibrils. The formed fibril bundles were non-uniform in size and shape, leaving massive voids between one another. Synthesis of cellulose derivatives like CAs provided sophisticated changes to the network structures through aggregation-induced phase separation, impacting the final microstructure and rigidity. The mass-heat transfer during film casting might also lead to the thermodynamic instability of cellulose-based materials, and phase separation occurs (Ferrarezi et al. 2013; Lee et al. 2006). These findings provided an insightful look into OPEFB's success in providing a desirable morphological trait, namely the highly fibrillated and web-like network in cellulose and CA synthesis, especially for heavy metal remediation membrane applications. Figure 2 also presents the SEM image of pristine ZnO particles prior to their incorporation into the CA system during membrane preparation. ZnO's spherical shape in nature was confirmed, as well as the agglomerates/aggregates and uneven separation (Muhammad et al. 2019; Mohan and Renjanadevi 2016). Its effectiveness as a filler in a hybrid organic–inorganic CA-based membrane system is further discussed.

To support the morphological findings, Fig. 3 showcases the EDS spectra for elemental analysis. Carbon (C) and oxygen (O) peaks were apparent in the spectra of both OPEFB-based and commercial cellulose. Once processed to be CAs, both cellulose spectra showed an appearance of the same elements, C and O, but with lower intensities. This shift proved the acetylation effect which reduced the number of both elements after the acetyl group introduction to replace the hydroxyl group of neat cellulose. The only difference between the spectra of OPEFB-based and commercial samples was the O peak being more intense than the C peak for OPEFB-based specimens. Meanwhile, the opposite was seen for commercial ones, as similarly found in another pristine CA study (Durthi and Rajulapati 2018). Different cellulose sources may offer different structural properties (Seddiqi et al. 2021). While for CA, the probable cause was the number of hydroxyl groups of cellulose repeat units replaced by acetyl groups. These elemental observations were further confirmed visually by the EDS field-of-view and mapping images (Fig. 3a, b) as a relation between chemical composition and structure, especially for membrane materials (Corneal et al. 2010; Qin et al. 2015).

Furthermore, the prospect of the ZnO-administered OPEFB CA system was discussed by analyzing Fig. 4**.** Through naked-eye detection, overall, all three CA-NMP-ZnO membranes looked identical, therefore, micrographic morphological observation was conducted next. As the solvent of choice, NMP possessed low volatility or vapor pressure. Its slow evaporation allowed the CA chains to undergo a lengthy relaxation process to form a membrane with a stable structure and well-packed configuration. The plasticization effect was also provided by NMP as it retained longer in the system and aided in weakening the CA region, forming porous regions (Lee et al. 2018; Tabe-Mohammadi et al. 2001). It can be noted through investigating the random pore distribution that the prepared membrane could be classified as an asymmetric membrane (Rajeswari et al. 2017). Despite the visible pinholes, cracks, and close-cave type voids, NMP-based CA membranes were proven to perform desirable separation ability with high selectivity through the walls of the close-cave structural model (Tabe-Mohammadi et al. 2001). The membrane surface smoothness was an improvement compared to those prepared with other more volatile solvents (e.g., acetone), including the after-use observation where the membrane shrinking and the visible voids disappearance were observed (Tabe-Mohammadi et al. 2001; W. G. Lee et al. 2018; Cindradewi et al. 2021), confirming the NMP-based membranes' longevity. Whereas, regarding ZnO, such inorganic material incorporation could affect thermodynamic/kinetics and increase suspension viscosity, yet at an excess amount might also decrease non-solvent diffusion and suppress the pores formation (Asiri et al. 2021; Shen et al. 2020; Alhalili et al. 2021; Balta et al. 2012), thus the optimum ratio is vital. ZnO particles could be seen blended and dispersed along the membranes' surface due to their hydrophilicity enhancer effect. Particularly at MMM 2 (0.75%ZnO; 90%NMP), the vastly interconnected network between blended ZnO and cellulose fibrils created more cavities/voids and increased roughness compared to MMM 1 (0.5%ZnO; 89%NMP), or essentially more pores (higher porosity) in smaller sizes and overall surface area (El-Noss et al. 2020; Chaurasia et al. 2010; Rajeswari et al. 2017; Gebru and Das 2017). However, at MMM 3 (1%ZnO; 91%NMP), ZnO clusters could be seen due to self-agglomeration/aggregation tendency after the naturally high surface energy of metal oxides (Liu et al. 2021a, b; Barnes et al. 2013), subsequently increasing pore sizes, as seen in other CA-metal oxide membrane studies (Ali et al. 2011; Alhalili et al. 2021; Gebru and Das 2017). A more in-depth investigation of membrane pores analysis is in the next section.

Porosity

In terms of membrane pores analysis, BET measures the adsorption aspect of adsorptive material relative to pressure. In this work, such findings would be crucial

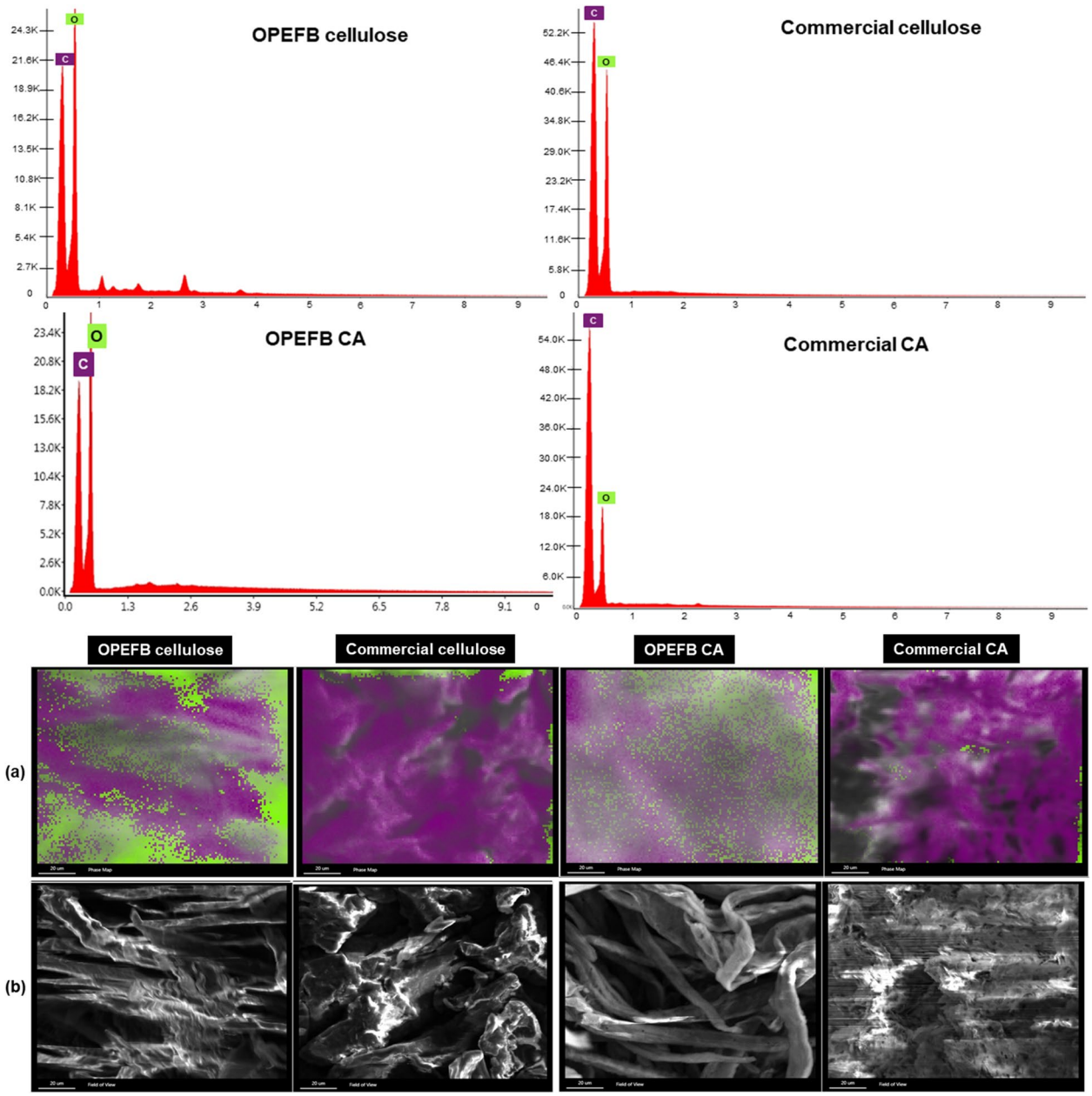


Fig. 3 EDS spectra and images (×1000, 20 µm scale): **a** field-of-view and **b** mapping of cellulose and CA

in determining the remediation performance of the fabricated OPEFB CA-NMP-ZnO membranes on its effectiveness in treating textile dyeing wastewater full of harmful dyes/chemicals. Pores quantitative analysis also would confirm the previously discussed morphological findings. Figure 5 shows the adsorption/desorption isotherm, explaining the relation between the relative pressure (P/P_o) and specific amount adsorbed (volume at standard temperature and pressure (STP) (cc/g)). The plots showed that the adsorption isotherm type may be measured as mixed types of I and IV (Tien 1994), similar to other CA membrane studies (Nemr et al. 2017; Ragab et al. 2023; Ali et al. 2024). This finding corresponds to IUPAC categories of micro-porosity (≤ 2 nm) and meso-porosity (2–50 nm) (Sing 1985), confirmed by pore statistics in Table 3 that the membranes' average radius ranged from 1.6 to 2.5 nm, comparable to other reports (Arthanareeswaran and Thanikaivelan 2010). Moreover, the obtained pore sizes were remarkable even compared to that of commercial membranes made of CA (Alves et al.

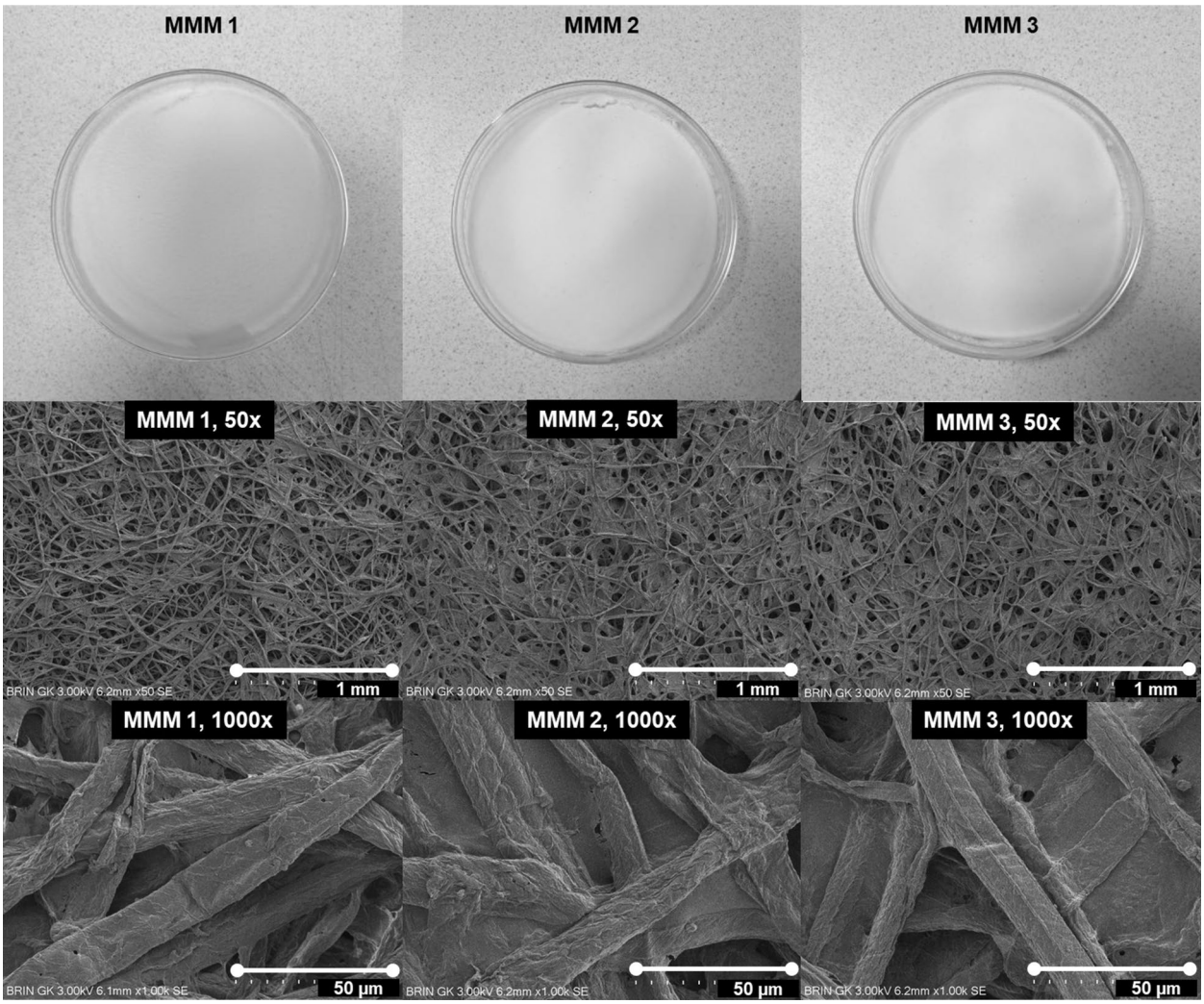


Fig. 4 Naked-eye detection and SEM images of OPEFB CA-NMP-ZnO membranes: ×50 (1 mm scale), ×1000 (50 µm scale)

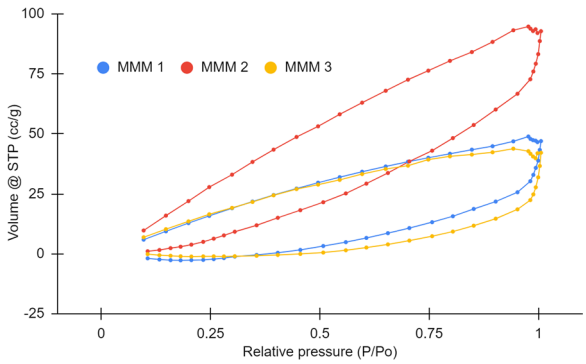


Fig. 5 Adsorption–desorption isotherm of OPEFB CA-NMP-ZnO membranes

Table 3 Porosity of OPEFB CA-NMP-ZnO membranes

Membrane		Radius, Dv(r) (nm)	Volume (cc/g)	Surface area (m^2/g)
MMM 1	Adsorption	1.9	0.08	30.7
	Desorption	1.7	0.06	39.1
MMM 2	Adsorption	1.6	0.15	72.1
	Desorption	1.7	0.12	80.8
MMM 3	Adsorption	2.5	0.06	16.7
	Desorption	1.7	0.05	35.2

2020), (both conventional and modified) polyvinylidene difluoride (PVDF), and polyether sulfone (PES) (Yang et al. 2022). As observed morphologically by SEM (Fig. 4), MMM 2 (0.75%ZnO; 90%NMP) indeed possessed the smallest adsorption radius (1.6 nm), while MMM 3 had

the largest (1%ZnO; 91%NMP) (2.5 nm). This evidenced the influence of optimum ratio and excessive addition of ZnO, as seen in other cases of metal oxide-doped CA membrane (Arthanareeswaran and Thanikaivelan 2010). Although, across different membranes, pores became smaller during desorption, where all showed identical desorption radius (1.7 nm). Similar to another modified CA membrane report (Ali et al. 2024), the aforementioned superior amount of formed pores and great surface area of MMM 2, as a positive impact of ZnO addition previously discussed in morphology analysis (Fig. 4), was confirmed with the acquired adsorption/desorption isotherm finding.

Mechanical properties

The effect of varying ratios of OPEFB CA-NMP-ZnO membranes on their mechanical properties is showcased in Fig. 6. MMM 2 (0.75%ZnO; 90%NMP) was the membrane with the best mechanical performance with the highest TS, E, and EAB valued at 1.78 MPa, 0.13 GPa, and 2.59%, respectively. This could be due to the high crystallinity of CA whose chains turn orientation in the direction of the stress when stretched, known as 'necking' (Pittarate et al. 2011; Ramakrishna 2005). It could also be due to the improved dense-layer thickness, CA–ZnO interaction, and the macro-voids suppression after the administered ZnO (Arthanareeswaran and Thanikaivelan 2010; Arthanareeswaran et al. 2008; Moghadassi et al. 2014). In contrast, the decline in all three mechanical properties, beginning at MMA 3, proved the effect of agglomerated excess NMP and ZnO and their eventually decreased distribution/dispersion within the CA structure as the matrix, acting as weak links. This phenomenon was similarly investigated in other doped CA membrane studies (Cindradewi et al. 2021; Wibowo et al. 2006; Arthanareeswaran and Thanikaivelan 2010; Arthanareeswaran et al. 2008). Such an influence of ratio and solvent on the mechanical stability of CA membranes has been reported (Stylianopoulos et al. 2012). Regardless, the obtained TS, E, and EAB values are comparable to those of previously researched CA membranes (Arthanareeswaran and Thanikaivelan 2010; Ghaffarian et al. 2015; Arthanareeswaran et al. 2008; Moghadassi et al. 2014).

Thermal property

Thermal stability is crucial when designing wastewater treatment membranes with a long-life span, especially when separating high-temperature (> 60 °C) streams (Zuo et al. 2020). Thermogravimetric findings through weight/mass (loss/gain) as a function of temperature/time could also be insightful in determining decomposition behavior and degradability (Brunšek et al. 2023). Figure 7 plots weight loss over changing temperature. Based on the produced TGA spectra Table 4 lists the samples' $T_{d,5\%}$, or the temperature at a 5%-weight loss, and %-weight at a final testing temperature of 500 °C.

The first content decomposed was the absorbed or loosely bound water and any volatile matter starting at temperatures ranging from 40–47 °C to 100 °C through evaporation, dehydration, or volatilization. However, the weight change was typically the least significant. The second yet most significant decomposition stage was on glucose rings in the cellulose chain and acetate functional groups for CAs, through pyrolysis at 260–360 °C leaving char/ash. The slow, final thermal-oxidative decomposition occurred at around 400 °C, marking the degraded elements' carbonization to ash (Yang et al. 2019; Ilyas et al. 2018; Abral et al. 2019; Araújo et al. 2018; Asrofi et al. 2018; Zhao et al. 2013; Liu et al. 2021a, b; Ali et al. 2011; Cindradewi et al. 2021). As also seen in a previous study (Fauziyyah et al. 2024), both OPEFB and

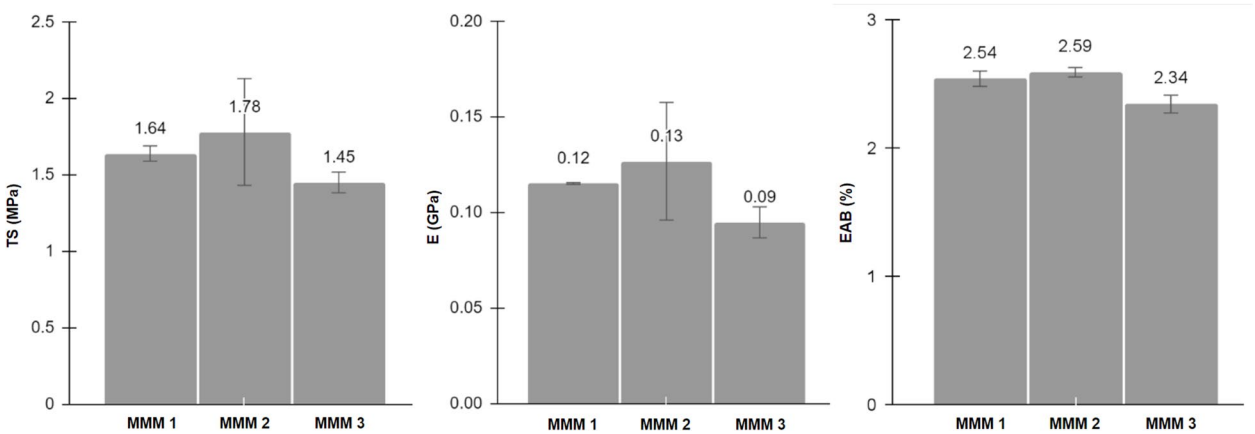


Fig. 6 Mechanical properties of OPEFB CA-NMP-ZnO membranes: tensile strength (TS), Young's modulus or (E), elongation-at-break (EAB)

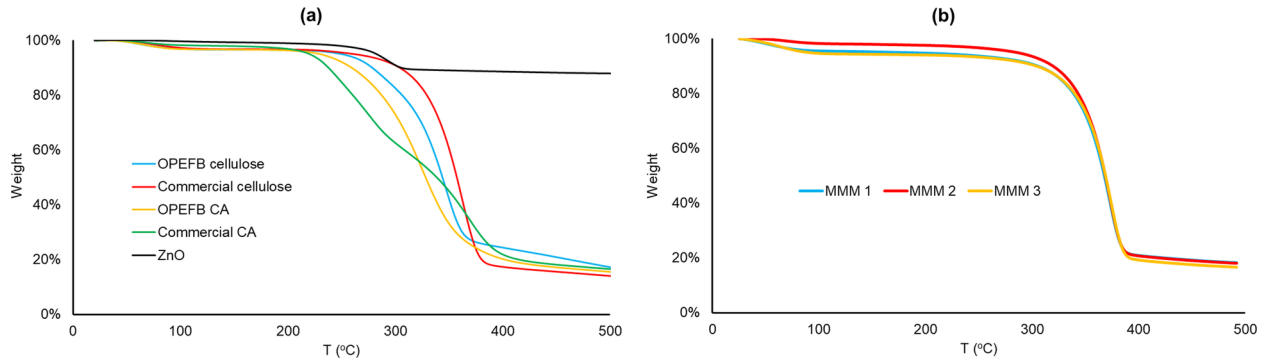


Fig. 7 TGA spectra of **a** cellulose, CA, ZnO; **b** OPEFB CA-NMP-ZnO membranes

Table 4 Degradation temperature and weight loss profile

Sample	$T_{d,5\%}$ (°C)	%W at 500 °C
OPEFB-cellulose	256	17
Commercial cellulose	270	14
OPEFB CA	235	16
Commercial CA	223	17
Pure ZnO	285	88
MMM 1	213	18
MMM 2	291	18
MMM 3	105	16

commercial CAs (223–235 °C) were proven to thermally degrade faster than neat cellulose (256–270 °C), as shown by their lower $T_{d,5\%}$. Such a decrease in thermal stability was due to the weakened hydrogen bonding post-acetylation as the hydroxyl groups were replaced by acetyl groups. There was also an influence from the crystalline structure fusion, random distribution of substitution (acetyl) groups, and chain low regularity or weak packing, making it thermally weaker (Barud et al. 2008).

In contrast, neat-ZnO powder, being an inorganic material with strong covalent bonds and lacking carbon/hydrogen atoms, performed distinctly superior thermal stability compared to any of the organic, cellulose-based specimens (Malakhov and Samsonov 1966; Johns et al. 1962). It is proven by not only its highest $T_{d,5\%}$ compared to all other samples but also most of its weight even at 500 °C (88%), unlike cellulose and CAs, whose %-weight only remained at 14–17% at the same temperature. Thus, ZnO incorporation into the CA system improved the thermal stability of the membranes (Asiri et al. 2021). In addition, as a solvent of choice, NMP possessed high thermal stability due to its high boiling point (Cindradewi et al. 2021). Hence, the remarkably high $T_{d,5\%}$ of MMM 2 (0.75%ZnO; 90%NMP) at 291 °C, since a strong CA-ZnO interaction required higher decomposition energy (A. Islam, Yasin, and Rehman 2014; Kim et al. 2010). The obtained value was comparable to that of a highly loaded CA-ZnO (10%) study (Alahmadi and Hussein 2022). This proved the positive thermal impact of not only ZnO incorporation, as seen in other CA-ZnO reports (Pérez-Silva et al. 2023; Alahmadi and Hussein 2022), but also the use of NMP. On the other hand, the extremely low $T_{d,5\%}$ of MMM 3 (1%ZnO; 91%NMP) at 105 °C was probably after the excess amount of added ZnO, causing particle agglomeration. This was similarly observed in other studies showing a negative effect on thermal stability by excessive ZnO addition in polypropylene (> 1%) (Esthappan et al. 2015) and polymethylmethacrylate (> 1%) (Hammani et al. 2018).

Remediation performance

The removal efficiency of Cu and Pb contained in wastewater in varying effluent concentrations by using CA-NMP-ZnO membranes, also referring to each of their porosity (Table 3), are highlighted in Fig. 8. Chemically, hydroxyl groups are the functional groups responsible for heavy metal ions adsorption by CA-based membranes (Liu and Bai 2006). Moreover, peaking of physical adsorption, membrane permeability was raised to a specific limit before lowering when the concentration of filler exceeded, marking the compactness occurring in the membrane structure (Idress et al. 2021; Cong et al. 2010). Generally, at lower effluent concentration (10%), it reached a complete remediation of Pb for all membranes. For both metal ions, the membranes performed exceptionally even at higher effluent concentrations (20%), as investigated in another report (Ji et al. 2012), where the amount of adsorbed heavy metal rose with the increase of the equilibrium concentration.

Interestingly, remediation performance generally dropped with the increase of NMP/ZnO content, possibly due to thickening issues. Such an accumulation led to difficulty for the Cu or Pb to diffuse within the internal

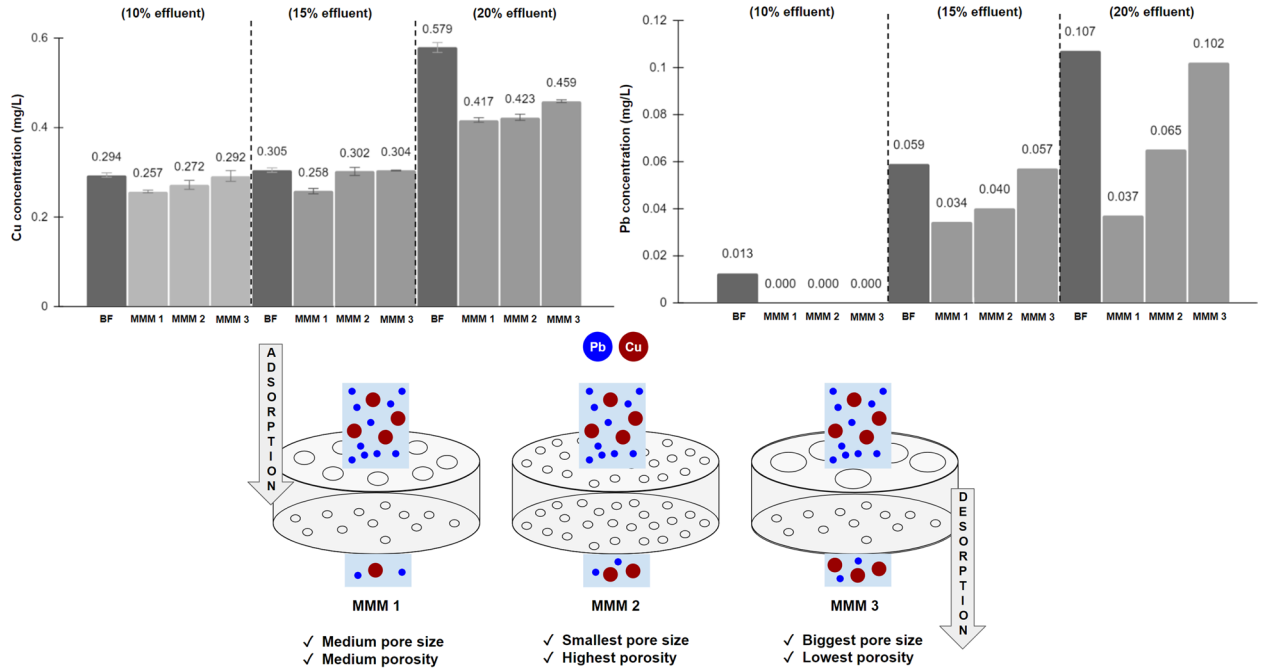


Fig. 8 Cu and Pb remediation performance of CA-NMP-ZnO membranes at varying effluent concentrations (BF: Before Filtration), and its illustration

and surface pores of the matrix (Gebru and Das 2017). This highlighted the collective influence of not only the membrane's pore characteristics (radius, volume/porosity, surface area) but also the size of the heavy metals. In general, removal efficiencies of the membranes were slightly superior for Pb compared to Cu, as reported in other cellulose-based membrane studies (Zhou et al. 2004; Ji et al. 2012; Gebru and Das 2017), possibly due to the bigger size/radius of Pb (Pb, 175 pm; Pb^{2+}, 119 pm) compared to Cu (Cu, 128 pm; Cu^{+}, 77 pm; Cu^{2+}, 73 pm) (Wells 1976). The trend was identical to that of a CA-TiO_2 membrane study (Gebru and Das 2017). The membrane pore characteristics mattered less when it came to Cu removal due to its smaller size, as shown by the almost identical remediation performance across three different membranes. In Pb removal, MMM 1 (0.5%ZnO; 89%NMP) was the best-performing membrane regardless of the effluent concentration, whose removal effectiveness reached 28% and 65% for Cu and Pb, respectively, at 20% effluent. Despite its smallest adsorption pore size (1.6 nm) among all membranes, MMM 2 (0.75%ZnO; 90%NMP) might possess too high of porosity, leading to heavy metal particles passing through the membrane too easily, resulting in the worsened remediation performance. Therefore, MMM 1, with its higher pore size (1.9 nm) yet optimum porosity, allowed effective adsorption of the heavy metals within the membrane network, hence its remarkable removal ability. The agglomerated ZnO at MMM 3 (1%ZnO; 91%NMP) hindered the diffusion of metal ions within the membrane system, hence the worst removal ability, as expected (Gebru and Das 2017).

It is worth noting that following the superior pore sizes (Table 3) even when compared to a few commercial CA, PVDF, and PES-based products (Alves et al. 2020; Yang et al. 2022), it could be assumed that the obtained membranes' absorption capacity and subsequent remediation performance would be competitive commercially (Mohammed et al. 2018). Rejection rates against specifically Cu and/or Pb of some other commercial membranes, e.g., NF 270 (Nayak et al. 2017; Kapepula et al. 2022), polyamide-based NF (Hanif et al. 2021), NE2540-70 (Cui et al. 2014), HFN-300 AR (Kumar et al. 2021), DL, DK, NTR-7450 (Wang et al. 2007), RO X-20, NF90 (Kapepula et al. 2022), have also been reported and deemed comparable to this work's findings. The cost-effectiveness of the synthesized CA membranes over commercial alternatives is another concern. Although cellulose isolation is time and energy-consuming, it could be considered more cost-effective than regenerating activated carbons, whose surface reactivation requires high temperature and energy (Marimuthu et al. 2023). Moreover, the offered antifouling feature in the developed MMMs could help reduce the operating cost for cleaning or replacement (El Batouti et al. 2021). Although, long-term implications (e.g., high cost, reduced flux, varying rejection rate per different filtration conditions, fouling, short service life, and weakened mechanical properties (Liu et al. 2021a, b; Li et al. 2022; Padhan et al. 2024))

might still linger, thus must be addressed. Like most similar studies, this report was based on laboratory-scale fabrication and application; thus, investigating the performance in pilot and bulk/industrial-scale is crucial in commercializing the designed membranes. The challenges include but are not limited to accessibility, renewability and recyclability, surface functionalization technological issues, biocompatibility to ensure long-term stability, standardization, and operational easiness (Vatanpour et al. 2022; Oprea and Voicu 2023; Kammakakam and Lai 2023; Padhan et al. 2024). Ultimately, aiming to comply with the textile (including 'batik') wastewater treatment standards, the respective national environmental regulations shall be considered. The Indonesian Ministry of Environment and Forestry Regulation No. 6 (2021) and the Malaysian-Environmental Quality Act 1974 have set maximum limits of 2.0 and 1.0 mg/L, respectively, for Cu; and 0.01 and 0.50 mg/L, respectively, for Pb (Ministry of Environment and Forestry of Republic of Indonesia 2021; Ministry of Natural Resources, Environment and Climate Change of Malaysia 2001). Therefore, it could be indicated that the resulting remediation performances were kept within the accepted values.

Conclusion

OPEFB was chosen as raw material in synthesizing CA intended as textile dyeing wastewater treatment. ZnO and NMP in varying concentrations as filler and solvent, respectively, were explored in terms of their impact on the CA membranes' characteristics. XRD of the prepared OPEFB-CA confirmed its high crystallinity even compared to a commercial product, as well as the fibrils web-like network by SEM–EDS. Once the OPEFB CA-NMP-ZnO membrane was prepared, its porous and smooth surface with an even dispersion of ZnO particles was also morphologically investigated, confirming the the NMP plasticizing effect. Mechanical and thermal stability improvement was also achieved. Overall, the membranes showcased a remarkable Cu and Pb remediation performance, even at high effluent concentrations. This work highlights the prospect of the use of a hefty yet notoriously underutilized biomass as a wastewater treatment alternative of the nations' signature textile industry.

Acknowledgements
The authors acknowledge the facilities, scientific and technical support from the Advanced Characterization Laboratories of BRIN Cibinong, Yogyakarta, and Serpong (Physics) through E-Layanan Sains BRIN. The authors gratefully acknowledge the financial support from Universiti Pertahanan Nasional Malaysia (UPNM). This work was also supported by the Kurita Water and Environment Foundation (Japan) through the Kurita Overseas Research Grant 2024 (Grant No. 24Pmy108 and PY/2024/01977; 24Pmy107 and PY/2024/01976).

Author contributions
Belladini Lovely: Formal analysis, Resources, Software, Visualization, Writing—original draft, Writing—review & editing. Hasna Amalia Fauziyyah, Shendy Krisdayanti: Data curation, Investigation. Muhamad Zakky Irsyada, Lisna Efiyanti: Visualization. Wara Dyah Pita Rengga, Novitri Hastuti: Conceptualization, Methodology, Resources, Supervision, Writing—review & editing. R.A. Ilyas, Mohd Faiz Norrrahim, Victor Feizal Knight, Supervision, Writing—review & editing. All authors read and approved the final manuscript.

Funding
This work was made possible by the Palm Oil Fund Management Agency of Republic of Indonesia (BPDPKS) grant, BRIN Post-Doctoral Fellow Program grant (140/II/HK/2024), Universiti Pertahanan National Malaysia fund, and Kurita Water and Environment Foundation (Japan) through the Kurita Overseas Research Grant 2024 (24Pmy108 and PY/2024/01977; 24Pmy107 and PY/2024/01976).

Availability of data and materials
Data will be provided upon request on a reasonable basis.

Declarations

Ethics approval and consent to participate
Not applicable.

Consent for publication
The authors give consent for publication.

Competing interests
The authors declare no competing interests.

Author details
[1]Research Center for Biomass and Bioproducts, National Research and Innovation Agency (BRIN), Bogor 16911, West Java, Indonesia. [2]Department of Chemical Engineering, Universitas Negeri Semarang, Semarang 50229, Central Java, Indonesia. [3]Department of Chemical Engineering, Faculty of Chemical and Energy Engineering, Universiti Teknologi Malaysia, 81310 Skudai, Johor, Malaysia. [4]Centre for Advanced Composite Materials (CACM), Universiti Teknologi Malaysia, 81310 Skudai, Johor, Malaysia. [5]Research Collaboration Center for Nanocellulose (BRIN - UNAND), Padang 25163, West Sumatra, Indonesia. [6]Research Centre for Chemical Defence, Defence Research Institute (DRI), Universiti Pertahanan Nasional Malaysia, Kuala Lumpur, Malaysia.

Received: 5 February 2025 Revised: 16 Apr 2025 Accepted: 25 April 2025
Published online: 19 June 2025

References

Abdelsamad AMA, Gad-Allah TA, Mahmoud FA, Badawy MI (2018) Enhanced photocatalytic degradation of textile wastewater using Ag/ZnO thin films. J Water Process Eng 25:88–95

Abdullah N, Sulaiman F (2013) The properties of the washed empty fruit bunches of oil palm. J Phys Sci 24(2):117–137

Abral H, Basri A, Muhammad F, Fernando Y, Hafizulhaq F, Mahardika M, Sugiarti E, Sapuan SM, IlyasStephane RAI (2019) A simple method for improving the properties of the sago starch films prepared by using ultrasonication treatment. Food Hydrocolloids 93:276–283

Ahmad FB, Zhang Z, Doherty WOS, O'Hara IM (2019) The outlook of the production of advanced fuels and chemicals from integrated oil palm biomass biorefinery. Renew Sustain Energy Rev 109:386–411

Alahmadi N, Hussein MA (2022) Hybrid nanocomposite membranes containing cellulose acetate @ CuO/ZnO for biological interest. J Market Res 21:4409–4418

Alhalili Z, Romdhani C, Chemingui H, Smiri M (2021) Removal of dithioterethiol (DTT) from water by membranes of cellulose acetate (AC) and AC doped ZnO and TiO_2 nanoparticles. J Saudi Chem Soc 25(8):101282

Ali M, Zafar M, Jamil T, Butt MTZ (2011) Influence of glycol additives on the structure and performance of cellulose acetate/zinc oxide blend membranes. Desalination 270(1):98–104

Ali AE, Elwardany RE, Mustafa AA, Shokry H (2024) Remediation of contaminated water using cellulose acetate membrane hybrid by sunflower seed shell–activated carbon. Biomass Convers Biorefin 5:5701–5717

Alventosa-deLara E, Barredo-Damas S, Zuriaga-Agustí E, Alcaina-Miranda MI, Iborra-Clar MI (2014) Ultrafiltration ceramic membrane performance during the treatment of model solutions containing dye and salt. Sep Purif Technol 129:96–105

Alves AA, Silva WE, Belian MF, Lins LSG, Galembeck A (2020) Bacterial cellulose membranes for environmental water remediation and industrial wastewater treatment. Int J Environ Sci Technol 17(9):3997–4008

Amin INHM, Nizam MHM (2016) Assessment of membrane fouling indices during removal of reactive dye from batik wastewater. J Water Reuse Desalin 6(4):505–514

Araújo IMS, Silva RR, Pacheco G, Lustri WR, Tercjak A, Gutierrez J, Júnior JRS et al (2018) Hydrothermal synthesis of bacterial cellulose-copper oxide nanocomposites and evaluation of their antimicrobial activity. Carbohyd Polym 179:341–349

Arthanareeswaran G, Thanikaivelan P (2010) Fabrication of cellulose acetate–zirconia hybrid membranes for ultrafiltration applications: performance, structure and fouling analysis. Sep Purif Technol 74(2):230–235

Arthanareeswaran G, Sriyamunadevi T, Raajenthiren M (2008) Effect of silica particles on cellulose acetate blend ultrafiltration membranes: part I. Sep Purif Technol 64(1):38–47

Asiri AM, Petrosino F, Pugliese V, Khan SB, Alamry KA, Alfifi SY, Marwani HM, Alotaibi MM, Algieri C, Chakraborty S (2021) Synthesis and characterization of blended cellulose acetate membranes. Polymers 14(1):4. https://doi.org/10.3390/polym14010004

Asrofi M, Abral H, Kasim A, Pratoto A, Mahardika M, Hafizulhaq F (2018) Mechanical properties of a water hyacinth nanofiber cellulose reinforced thermoplastic starch bionanocomposite: effect of ultrasonic vibration during processing. Fibers Polym 6(2):40

ASTM International (2022) Test method for tensile properties of plastics. ASTM International, West Conshohocken, PA

Azha SF, Ismail S (2021) Feasible and economical treatment of real hand-drawn batik/textile effluent using Zwitterionic adsorbent coating: removal performance and industrial application approach. J Water Process Eng 41:102093

Balta S, Sotto A, Luis P, Benea L, Van der Bruggen B, Kim J (2012) A new outlook on membrane enhancement with nanoparticles: the alternative of ZnO. J Membr Sci 389:155–161

Barnes RJ, Molina R, Jianbin Xu, Dobson PJ, Thompson IP (2013) Comparison of TiO_2 and ZnO nanoparticles for photocatalytic degradation of methylene blue and the correlated inactivation of gram-positive and gram-negative bacteria. J Nanoparticle Res 15(2):1432

Barud HS, de Araújo AM, Júnior DB, Santos RMN, de Assunção CS, Meireles DA, Cerqueira GR, Filho CA, Ribeiro YM, Ribeiro SJL (2008) Thermal behavior of cellulose acetate produced from homogeneous acetylation of bacterial cellulose. Thermochim Acta 471(1):61–69

Ben Dassi R, Chamam B, Méricq JP, Faur C, El Mir L, Trabelsi I, Heran M (2021) Novel polyvinylidene fluoride/lead-doped zinc oxide adsorptive membranes for enhancement of the removal of reactive textile dye. Int J Environ Sci Technol 18(9):2793–2804

Brunšek R, Kopitar D, Schwarz I, Marasović P (2023) Biodegradation properties of cellulose fibers and PLA biopolymer. Polymers 15(17):3532. https://doi.org/10.3390/polym15173532

Budiyanto S, Purnaweni H, Sunoko HR (2018) Environmental analysis of the impacts of batik waste water polution on the quality of dug well water in the Batik industrial center of Jenggot Pekalongan City. E3S Web Conf 31:09008

Buthiyappan A, Raman AAA, Daud WMA (2016) Development of an advanced chemical oxidation wastewater treatment system for the batik industry in Malaysia. RSC Adv 6(30):25222–25241

Chang SH (2014) An overview of empty fruit bunch from oil palm as feedstock for bio-oil production. Biomass Bioenerg 62:174–181

Chaurasia V, Chand N, Bajpai SK (2010) Water sorption properties and antimicrobial action of zinc oxide nanoparticles-loaded cellulose acetate films. J Macromol Sci Part A Pure Appl Chem 47(4):309–317

Cindradewi AW, Bandi R, Park C-W, Park J-S, Lee E-A, Kim J-K, Kwon G-J, Han S-Y, Lee S-H (2021) Preparation and characterization of cellulose acetate film reinforced with cellulose nanofibril. Polymers 13(17):2990. https://doi.org/10.3390/polym13172990

Cong H-P, He J-J, Yang Lu, Shu-Hong Yu (2010) Water-soluble magnetic-functionalized reduced graphene oxide sheets. In situ synthesis and magnetic resonance imaging applications. Small 6(2):169–173

Corley RHV, Tinker PBH (2008) The oil palm. Wiley, Chichester

Corneal LM, Masten SJ, Davies SHR, Tarabara VV, Byun S, Baumann MJ (2010) AFM, SEM and EDS characterization of manganese oxide coated ceramic water filtration membranes. J Membr Sci 360(1–2):292–302

Cui Y, Ge Q, Liu X-Y, Chung T-S (2014) Novel forward osmosis process to effectively remove heavy metal ions. J Membr Sci 467:188–194

Dahnum D, Tasum SO, Triwahyuni E, Nurdin M, Abimanyu H (2015) Comparison of SHF and SSF processes using enzyme and dry yeast for optimization of bioethanol production from empty fruit bunch. Energy Procedia 68:107–116

Daicho K, Saito T, Fujisawa S, Isogai A (2018) The crystallinity of nanocellulose: dispersion-induced disordering of the grain boundary in biologically structured cellulose. ACS Appl Nano Mater 1(10):5774–5785

Dalimin MN (1995) Renewable energy update: Malaysia. Renew Energy 6(4):435–439

Daud WRW, Djuned FM (2015) Cellulose acetate from oil palm empty fruit bunch via a one step heterogeneous acetylation. Carbohydrate Polym. 132:252–260

Desa AL, Hairom NHH, Ng LY, Ng CY, Ahmad MK, Mohammad AW (2019) Industrial textile wastewater treatment via membrane photocatalytic reactor (MPR) in the presence of ZnO-PEG nanoparticles and tight ultrafiltration. J Water Process Eng 31(100872):100872

Djuned FM, Asad M, Mohamad Ibrahim MN (2014) Synthesis and characterization of cellulose acetate from TCF oil palm empty fruit bunch pulp. BioResources. https://doi.org/10.15376/biores.9.3.4710-4721

Douna I, Farrukh S, Pervaiz E, Hussain A, Fan XF, Salahuddin Z (2023) Blending of ZnO Nanorods in cellulose acetate mixed matrix membrane for enhancement of CO_2 permeability. J Polym Environ 31(6):2549–2565

Durthi CP, Rajulapati SB (2018) Studies on removal of arsenic using cellulose acetate–zinc oxide nanoparticle mixed matrix membrane. Int Nano Lett 8:201–211

El Batouti M, Al-Harby NF, Elewa MM (2021) A review on promising membrane technology approaches for heavy metal removal from water and wastewater to solve water crisis. Water 13(22):3241

El Nemr A, Ragab S, El Sikaily A (2017) Rapid synthesis of cellulose triacetate from cotton cellulose and its effect on specific surface area and particle size distribution. Iran Polym J 26(4):261–272

El-Noss M, Isawi H, Shawky HA, Gomaa MA, Abdel-Mottaleb MSA (2020) Improvement of cellulose acetate forward osmosis membrane performance using zinc oxide nanoparticles. Desalin Water Treat 193:19–33

Esthappan SK, Nair AB, Joseph R (2015) Effect of crystallite size of zinc oxide on the mechanical, thermal and flow properties of polypropylene/zinc oxide nanocomposites. Composites Part B Engineering 69:145–53

Etafo NO, Bamidele MO, Bamisaye A, Alli YA (2024) Revolutionizing photocatalysis: unveiling efficient alternatives to titanium (IV) oxide and zinc oxide for comprehensive environmental remediation. J Water Process Eng 62:105369

Fan X, Liu Z-W, Jian Lu, Liu Z-T (2009) Cellulose triacetate optical film preparation from ramie fiber. Ind Eng Chem Res 48(13):6212–6215

Fauziyyah AHA, Krisdayanti S, Suwandi LAC, Irsyada MZ, Faizin MN, Hastuti N, Rengga WDP (2024) Synthesis and characterization of cellulose acetate from oil palm empty fruit bunches (OPEFB) as membrane material. E3S Web Conf 576:06010

Febriasari A, Suhartini M, Rahmawati BH, Anggarini NH, Yunus AL, Hermana RF et al (2024) Enhancing the CO_2/CH_4 separation properties of cellulose acetate membranes using polyethylene glycol methyl ether acrylate radiation grafting. J Polym Environ 32(10):4855–4868

Ferrarezi MMF, Rodrigues GV, Felisberti MI, do Carmo Gonçalves M (2013) Investigation of cellulose acetate viscoelastic properties in different solvents and microstructure. Eur Polym J 49(9):2730–2737

Filho GR, da Cruz SF, Pasquini D, Cerqueira DA, de Souza Prado V, de Assunção RMN (2000) Water flux through cellulose triacetate films produced from heterogeneous acetylation of sugar cane Bagasse. J Membrane Sci 177(1):225–31

Fischer S, Thümmler K, Volkert B, Hettrich K, Schmidt I, Fischer K (2008) Properties and applications of cellulose acetate. Macromol Symp 262(1):89–96

Franklin NM, Rogers NJ, Apte SC, Batley GE, Gadd GE, Casey PS (2007) Comparative toxicity of nanoparticulate ZnO, bulk ZnO, and $ZnCl_2$ to a freshwater microalga (Pseudokirchneriella Subcapitata): the importance of particle solubility. Environ Sci Technol 41(24):8484–8490

Gebru KA, Das C (2017) Removal of Pb (II) and Cu (II) ions from wastewater using composite electrospun cellulose acetate/titanium Oxide (TiO_2) adsorbent. J Water Process Eng 16:1–13

Geng A (2013) Conversion of oil palm empty fruit bunch to biofuels. Intechopen, Croatia

Ghaee A, Shariaty-Niassar M, Barzin J, Matsuura T, Ismail AF (2016) Preparation of chitosan/cellulose acetate composite nanofiltration membrane for wastewater treatment. Desalin Water Treat 57(31):14453–14460

Ghaffarian V, Mousavi SM, Bahreini M (2015) Effect of blend ratio and coagulation bath temperature on the morphology, tensile strength and performance of cellulose acetate/poly(butylene succinate) membranes. Desalin Water Treat 54(2):473–480

Ghaly A, Ananthashankar R, Alhattab M, Ramakrishnan V (2013) Production, characterization and treatment of textile effluents: a critical review. J Chem Eng Process Technol 05:01. https://doi.org/10.4172/2157-7048.1000182

Guo MY, Fung MK, Fang F, Chen XY, Ng AMC, Djurišić AB, Chan WK (2011) ZnO and TiO_2 1D nanostructures for photocatalytic applications. J Alloy Compd 509(4):1328–1332

Hammani S, Barhoum A, Bechelany M (2018) Fabrication of PMMA/ZnO nanocomposite: effect of high nanoparticles loading on the optical and thermal properties. J Mater Sci 53(3):1911–1921

Hanif A, Ali S, Hanif MA, Rashid U, Bhatti HN, Asghar M, Alsalme A, Giannakoudakis DA (2021) A novel combined treatment process of hybrid biosorbent–nanofiltration for effective Pb(II) removal from wastewater. Water 13(23):3316

Hassan A, Salema AA, Ani FN, Bakar AA (2010) A review on oil palm empty fruit bunch fiber-reinforced polymer composite materials. Polym Compos 31(12):2079–2101

Hassan H, Shokry MF, Elkady AA, Farghali AM, Mohamed SalemAbd El-Hamid AAI (2017) Fabrication of novel magnetic zinc oxide cellulose acetate hybrid nano-fiber to be utilized for phenol decontamination. J Taiwan Inst Chem Eng 78:307–316

Hong J, He Y (2014) Polyvinylidene fluoride ultrafiltration membrane blended with nano-ZnO particle for photo-catalysis self-cleaning. Desalination 332(1):67–75

Hornung A (2014) Transformation of biomass theory to practice. Wiley, Chichester

Hua M, Zhang S, Pan B, Zhang W, Lv L, Zhang Q (2012) Heavy metal removal from water/wastewater by nanosized metal oxides: a review. J Hazard Mater 211–212:317–31

Idress H, Zaidi SZJ, Sabir A, Shafiq M, Khan RU, Harito C, Hassan S, Walsh FC (2021) Cellulose acetate based complexation-NF membranes for the removal of Pb(II) from waste water. Sci Rep 11(1):1806

Ilyas RA, Sapuan SM, Ishak MR, Zainudin ES (2018) Development and characterization of sugar palm nanocrystalline cellulose reinforced sugar palm starch bionanocomposites. Carbohyd Polym 202:186–202

Islam A, Yasin T, ur Rehman I (2014) Synthesis of hybrid polymer networks of irradiated chitosan/poly(vinyl alcohol) for biomedical applications. Radiat Phys Chem 96:115–119

Islam MD, Uddin FJ, Rashid TU, Shahruzzaman M (2023) Cellulose acetate-based membrane for wastewater treatment—a state-of-the-art review. Mater Adv 4(18):4054–4102

Istirokhatun T, Susanto H, Budihardjo MA, Septiyani E, Wibowo AR, Karamah EF (2021) Treatment of batik industry wastewater plant effluent using nanofiltration. Int J Technol 12(4):770

Jamaluddin NS, Alias NH, Jaafar J, Othman NH, Sadaki S, Marpani F, Lau WJ, Aziz MHA (2022) Exploring potential of adsorptive-photocatalytic molybdenum disulphide/polyacrylonitrile (MoS_2/PAN) nanofiber coated cellulose acetate (CA) membranes for treatment of wastewater. J Polym Environ 30(12):5290–5300

Javed F, Tariq MF, Ikhlaq A, Munir HMS, Altaee A (2025) Remediation of textile wastewater by hybrid technique using ZIF-67 catalyzed ozonation coupled with electrocoagulation. J Water Process Eng 69:106604

Jebelli F, Hasheminejad H, Mousaabadi KZ (2024) Efficient photocatalytic decolorization of textile wastewater using Fe-Mo LDH/ZnO nanocomposite: a sustainable approach for environmental remediation. J Water Process Eng 59:104981

Ji F, Li C, Tang B, Xu J, Lu G, Liu P (2012) Preparation of cellulose acetate/zeolite composite fiber and its adsorption behavior for heavy metal ions in aqueous solution. Chem Eng J 209:325–33

Johns IB, McElhill EA, Smith JO (1962) Thermal stability of organic compounds. I&EC Product Res Dev 1(1):2–6

Jorge AMS, Athira KK, Alves MB, Gardas RL, Pereira JFB (2023) Textile dyes effluents: a current scenario and the use of aqueous biphasic systems for the recovery of dyes. J Water Process Eng 55:104125

Juliani A (2021) Heavy metal characteristics of wastewater from batik industry in Yogyakarta Area, Indonesia. Int J Geomate 20:80. https://doi.org/10.21660/2021.80.6271

Kalia S, Dufresne A, Cherian BM, Kaith BS, Avérous L, Njuguna J, Nassiopoulos E (2011) Cellulose-based bio- and nanocomposites: a review. Int J Polym Sci 2011:1–35

Kamble AR, Patel CM, Murthy ZVP (2021) A review on the recent advances in mixed matrix membranes for gas separation processes. Renew Sustain Energy Rev 145:111062

Kammakakam I, Lai Z (2023) Next-generation ultrafiltration membranes: a review of material design, properties, recent progress, and challenges. Chemosphere 316:137669

Kapepula L, Vercus MG, Alvarez VS, Sefidi EB, Tamungang N, Ndikumana T, Musibono D-D, Van Der Bruggen B, Luis P (2022) Evaluation of commercial reverse osmosis and nanofiltration membranes for the removal of heavy metals from surface water in the Democratic Republic of Congo. Clean Technol 4(4):1300–1316

Karthik P, Rajesh J, Ravichandran S (2024) Comprehensive review on the advancement of transition metal oxides infused cellulose acetate nanocomposites for the photocatalytic degradation of emerging pollutants. J Water Process Eng 66:106010

Kerdsuwan S, Laohalidanond K (2011) Renewable energy from palm oil empty fruit bunch. Intechopen, Croatia

Kim U-J, Eom SH, Wada M (2010) Thermal decomposition of native cellulose: influence on crystallite size. Polym Degrad Stab 95(5):778–781

Kono H, Numata Y, Nagai N, Erata T, Takai M (1999) Studies of the series of cellooligosaccharide peracetates as a model for cellulose triacetate by 13C CP/MAS NMR spectroscopy and X-ray analyses. Carbohyd Res 322(3):256–263

Kumar J, Joshi H, Malyan SK (2021) Removal of copper, nickel, and zinc ions from an aqueous solution through electrochemical and nanofiltration membrane processes. Appl Sci 12(1):280

Lai DS, Osman AF, Adnan SA, Ibrahim I, Alrashdi AA, Salimi MNA, Ul-Hamid A (2021) On the use of OPEFB-derived microcrystalline cellulose and nano-bentonite for development of thermoplastic starch hybrid biocomposites with improved performance. Polymers 13(6):897. https://doi.org/10.3390/polym13060897

Law K-N, Daud WRW, Arniza G (2007) Morphological and chemical nature of fiber strands of oil palm empty-fruit-bunch (OPEFB). BioResources 2(3):351–362. https://doi.org/10.15376/biores.2.4.351-362

Lee JH, Kim BS, Lee JC, Park S (2005) Removal of Cu^{++} ions from aqueous Cu-EDTA solution using ZnO nanopowder. Mater Sci Forum 486–487:510–513

Lee H, Chaudhuri SR, Krantz WB, Hwang S-T (2006) A model for evaporative casting of polymeric membranes incorporating convection due to density changes. J Membr Sci 284(1):161–172

Lee WG, Kim DY, Kang SW (2018) Porous cellulose acetate by specific solvents with water pressure treatment for applications to separator and membranes. Macromol Res 26(7):630–633

Lestari S, Sudarmadji, Tandjung SD, Santosa SJ (2019) Improvement of batik wastewater quality using biosorption process. IOP Conf Series Earth Environ Sci 256(1):012047

Li S, Wang X, Guo Y, Jiwen Hu, Lin S, Yuanyuan Tu, Chen L, Ni Y, Huang L (2022) Recent advances on cellulose-based nanofiltration membranes and their applications in drinking water purification: a review. J Clean Prod 333:130171

Liang S, Xiao K, Mo Y, Huang X (2012) A novel ZnO nanoparticle blended polyvinylidene fluoride membrane for anti-irreversible fouling. J Membr Sci 394–395:184–192

Liang C-Z, Sun S-P, Li F-Y, Ong Y-K, Chung T-S (2014) Treatment of highly concentrated wastewater containing multiple synthetic dyes by a

combined process of coagulation/flocculation and nanofiltration. J Membr Sci 469:306–315
Liu C, Bai R (2006) Adsorptive removal of copper ions with highly porous chitosan/cellulose acetate blend hollow fiber membranes. J Membr Sci 284(1–2):313–322
Liu G-Q, Pan X-J, Li J, Li C, Ji C-L (2021a) Facile preparation and characterization of anatase TiO_2/nanocellulose composite for photocatalytic degradation of methyl orange. J Saudi Chem Soc 25(12):101383
Liu Y, Liu H, Shen Z (2021b) Nanocellulose based filtration membrane in industrial waste water treatment: a review. Materials 14(18):5398
Liu Y, Hongqiao Fu, Zhang W, Liu H (2022) Effect of crystalline structure on the catalytic hydrolysis of cellulose in subcritical water. ACS Sustain Chem Eng 10(18):5859–5866
Loh SK (2017) The potential of the Malaysian oil palm biomass as a renewable energy source. Energy Convers Manage 141:285–298
Mahlangu OT, Nackaerts R, Thwala JM, Mamba BB, Verliefde ARD (2017) Hydrophilic fouling-resistant GO-ZnO/PES membranes for wastewater reclamation. J Membr Sci 524:43–55
Malakhov YS, Samsonov GV (1966) Regularities governing the thermal stability of oxides of the transition metals. Soviet Powder Metall Metal Ceram 5(12):981–986
Mani A, Meikandaan TP, Gowrishankar PG, Kanchanabhan TE (2019) A study on treatment of industrial effluent (dyeing) using Moringa Oleifera, Tamarina Indica as Coagulants. Int J Civil Eng Technol 10(1):2796–2811
Marimuthu T, Chee CY, Sulaiman NMN (2023) A review on the use of cellulose nanomaterials for wastewater remediation of heavy metal ions. Int J Environ Sci Technol 20(3):3421–3436
Masupha TM (2008) Water management at a textile industry: a case study in Lesotho. Edited by Francois Friend. University of Pretoria (South Africa). https://repository.up.ac.za/handle/2263/24062
Megashah LN, Ariffin H, Zakaria MR, Hassan MA (2018) Multi-step pretreatment as an eco-efficient pretreatment method for the production of cellulose nanofiber from oil palm empty fruit bunch. Asia Pac J Mol Biol Biotechnol 26:1–8
Miao X, Lin J, Bian F (2020) Utilization of discarded crop straw to produce cellulose nanofibrils and their assemblies. J Bioresour Bioprod 5(1):26–36
Ministry of Environment and Forestry of Republic of Indonesia (2021) Tata Cara Dan Persyaratan Pengelolaan Limbah Bahan Berbahaya Dan Beracun. 6. https://jdih.menlhk.go.id/new2/uploads/files/2021pmlhk006_menlhk_06082021104752.pdf
Moghadassi AR, Rajabi Z, Hosseini SM, Mohammadi M (2014) Fabrication and modification of cellulose acetate based mixed matrix membrane: gas separation and physical properties. J Ind Eng Chem 20(3):1050–1060
Mohammed N, Grishkewich N, Tam KC (2018) Cellulose nanomaterials: promising sustainable nanomaterials for application in water/wastewater treatment processes. Environ Sci Nano 5(3):623–658
Mohan AC, Renjanadevi B (2016) Preparation of Zinc oxide nanoparticles and its characterization using scanning electron microscopy (SEM) and X-ray diffraction (XRD). Procedia Technol 24:761–766
Muhammad W, Ullah N, Haroon M, Abbasi BH (2019) Optical, morphological and biological analysis of zinc oxide nanoparticles (ZnO NPs) using Papaver somniferum L. RSC Adv 9(51):29541–29548
Mutsaers HJW (2019) The challenge of the oil palm: using degraded land for its cultivation. Outlook Agric 48(3):190–197
Nasouri K (2019) Fabrication of lightweight and flexible cellulose acetate composite nanofibers for high-performance ultra violet protective materials. Polym Compos 40(8):3325–3332
Nayak V, Jyothi MS, Geetha Balakrishna R, Padaki M, Deon S (2017) Novel modified poly vinyl chloride blend membranes for removal of heavy metals from mixed ion feed sample. J Hazard Mater 331:289–299
Ngulube KF, Abdelhaleem A, Fujii M, Nasr M (2024) Synthesis of smart ZnO@$Mg(OH)_2$ core–shell nanocomposite and its application for methylene blue photocatalytic degradation: life cycle sustainability assessment and techno-economics. J Water Process Eng 64:105605
Nuhnen A, Janiak C (2021) Mixed-matrix membranes. In: Abadie MJM, Pinteala M, Rotaru A (eds) New trends in macromolecular and supramolecular chemistry for biological applications. Springer International Publishing, Cham, pp 87–113
Nurhadi B, Angeline A, Sukri N, Masruchin N, Arifin HR, Saputra RA (2022) Characteristics of microcrystalline cellulose from nata de coco: hydrochloric acid versus maleic acid hydrolysis. J Appl Polym Sci 139(5):51576
Odubanjo GO, Oyetibo GO, Ilori MO (2021) Ecological risks of heavy metals and microbiome taxonomic profile of a freshwater stream receiving wastewater of textile industry. Front Environ Sci Eng China 9:554490. https://doi.org/10.3389/fenvs.2021.554490
Oprea M, Voicu SI (2023) Cellulose acetate-based materials for water treatment in the context of circular economy. Water 15(10):1860
Padhan B, Ryoo W, Patel M, Dash JK, Patel R (2024) Cutting-edge applications of cellulose-based membranes in drug and organic contaminant removal: recent advances and innovations. Polymers 16(20):2938
Panchal P, Ogunsona E, Mekonnen T (2018) Trends in advanced functional material applications of nanocellulose. Processes 7(1):10
Park S, Baker JO, Himmel ME, Parilla PA, Johnson DK (2010) Cellulose crystallinity index: measurement techniques and their impact on interpreting cellulase performance. Biotechnol Biofuels 3:10
Pérez-Silva I, Páez-Hernández ME, Ibarra IS, Camacho-Mendoza RL (2023) Evaluation of the hybrid membrane of ZnO particles supported in cellulose acetate for the removal of lead. Membranes 13(2):123
Pittarate C, Yoovidhya T, Srichumpuang W, Intasanta N, Wongsasulak S (2011) Effects of poly(ethylene Oxide) and ZnO nanoparticles on the morphology, tensile and thermal properties of cellulose acetate nanocomposite fibrous film. Polym J 43(12):978–986
Qin L, Mergos IA, Verweij H (2015) Obtaining accurate cross-section images of supported polymeric and inorganic membrane structures. J Membr Sci 476:194–199
Ragab S, El Sikaily A, El Nemr A (2023) Fabrication of dialysis membrane from cotton giza 86 cellulose di-acetate prepared using AC2O and $NiCl_2$ as a new catalyst. Sci Rep 13(1):2276
Rahmaniah G, Mahdi C, Safitri A (2019) Biosorption of synthetic dye from batik wastewater using trichoderma viride Immobilized on Ca-alginate. J Phys: Conf Ser 1374(1):012007
Rajeswari A, Vismaiya S, Pius A (2017) Preparation, characterization of nano ZnO-blended cellulose acetate-polyurethane membrane for photocatalytic degradation of dyes from water. Chem Eng J 313:928–937
Ramakreshnan L, Rajandra A, Aghamohammadi N, Fong CS, Nalatambi S (2020) A preliminary insight into the environmental awareness of community in the vicinity of batik manufacturing Units in Kelantan, Malaysia. GeoJournal 85(6):1745–1753
Ramakrishna S (2005) An introduction to electrospinning and nanofibers. World Scientific Publishing, Singapore. https://doi.org/10.1142/9789812567611
Rana J, Goindi G, Kaur N, Krishna S, Kakati A (2022) Synthesis and application of cellulose acetate-acrylic acid-acrylamide composite for removal of toxic methylene blue dye from aqueous solution. J Water Process Eng 49(103102):103102
Rashid MM, Shen X, Islam SR, Mizan RA, Hong Y (2022) Sono-synthesis of cellulose-TiO_2 nanocomposite adsorbent for fast cleaning of anionic dyes containing wastewater. J Water Process Eng 47:102799
Rashidi HR, Nik Sulaiman NM, Hashim NA (2012) Batik industry synthetic wastewater treatment using nanofiltration membrane. Procedia Eng 44:2010–2012
Razali N, Hossain MS, Taiwo OA, Ibrahim M, Nadzri NWM, Razak N, Rawi NFM, Mahadar MM, Kassim MHM (2017) Influence of acid hydrolysis reaction time on the isolation of cellulose nanowhiskers from oil palm empty fruit bunch microcrystalline cellulose. Bioresources 12(3):6773–6788. https://doi.org/10.15376/biores.12.3.6773-6788
Rezagama A, Sutrisno E, Handayani DS (2020) Pollution model of batik and domestic wastewater on river water quality. IOP Conf Series Earth Environ Sci 448(1):012074
Ritchie H, Spooner F, Roser M (2023) Forests and deforestation. Our World in Data, December. https://ourworldindata.org/forests-and-deforestation
Seddiqi H, Oliaei E, Honarkar H, Jin J, Geonzon LC, Bacabac RG, Klein-Nulend J (2021) Cellulose and its derivatives: towards biomedical applications. Cellulose (London, England) 28(4):1893–1931
Segal L, Creely JJ, Martin AE, Conrad CM (1959) An empirical method for estimating the degree of crystallinity of native cellulose using the X-ray diffractometer. Text Res J 29(10):786–794
Sharma R, Bisen DP, Shukla U, Sharma BG (2012) X-ray diffraction: a powerful method of characterizing nanomaterials. Recent Res Sci Technol 4(8):77–79

Sheikh M, Pazirofteh M, Dehghani M, Asghari M, Rezakazemi M, Valderrama C, Cortina J-L (2020) Application of ZnO nanostructures in ceramic and polymeric membranes for water and wastewater technologies: a review. Chem Eng J 391:123475
Shen L, Bian X, Xiaofeng Lu, Shi L, Liu Z, Chen L, Hou Z, Fan K (2012) Preparation and characterization of ZnO/polyethersulfone (PES) hybrid membranes. Desalination 293:21–29
Shen L, Huang Z, Liu Y, Li R, Yanchao Xu, Jakaj G, Lin H (2020) Polymeric membranes incorporated with ZnO nanoparticles for membrane fouling mitigation: a brief review. Front Chem 8:224
Shenvi S, Ismail AF, Isloor AM (2014) Enhanced permeation performance of cellulose acetate ultrafiltration membranes by incorporation of sulfonated poly(1,4-phenylene ether ether sulfone) and poly(styrene-co-maleic anhydride). Ind Eng Chem Res 53(35):13820–13827
Shukla G, Rani M, Shanker U, Baigenzhenov O, Hosseini-Bandegharaei A (2025) Recent advances and prospects on the R-GO incorporated metal oxide semiconductors for enhanced photo-adsorptive abatement of toxic wastewater pollutants. J Water Process Eng 69:106630
Sing KSW (1985) Reporting physisorption data for gas/solid systems with special reference to the determination of surface area and porosity (recommendations 1984). Pure Appl Chem Chim Pure Appl 57(4):603–619
Sivakumar M, Malaisamy R, Sajitha CJ, Mohan D, Mohan V, Rangarajan R (1999) Ultrafiltration application of cellulose acetate–polyurethane blend membranes. Eur Polym J 35(9):1647–1651
Slama HB, Bouket AC, Pourhassan Z, Alenezi FN, Silini A, Cherif-Silini H, Oszako T, Luptakova L, Golińska P, Belbahri L (2021) Diversity of synthetic dyes from textile industries, discharge impacts and treatment methods. NATO Adv Sci Inst Ser E Appl Sci 11(14):6255
Stylianopoulos T, Kokonou M, Michael S, Tryfonos A, Rebholz C, Odysseos AD, Doumanidis C (2012) Tensile mechanical properties and hydraulic permeabilities of electrospun cellulose acetate fiber meshes. J Biomed Mater Res Part B Appl Biomater 100(8):2222–2230
Sulaiman F, Abdullah N, Gerhauser H, Shariff A (2010) A perspective of oil palm and its wastes. J Phys Sci 21(1):67–77
Susi S, Ainuri M, Wagiman W, Falah MAF (2023) High-yield alpha-cellulose from oil palm empty fruit bunches by optimizing thermochemical delignification processes for use as microcrystalline cellulose. Int J Biomater 2023:9169431
Suwantong O, Supaphol P (2015) Applications of cellulose acetate nanofiber mats. In: Pandey JK, Takagi H, Nakagaito AN, Kim H-J (eds) Handbook of polymer nanocomposites. Processing, performance and application: volume C: Polymer nanocomposites of cellulose nanoparticles. Springer, Berlin, pp 355–368
Syamani FA (2020) Cellulose-based membrane for adsorption of dye in batik industry wastewater. Int J Hydrol 4(6):281–283
Tabe-Mohammadi A, Garcia JP, Villaluenga HJ, Kim TC, Rauw V (2001) Effects of polymer solvents on the performance of cellulose acetate membranes in methanol/methyl tertiary butyl ether separation. J Appl Polym Sci 82(12):2882–2895
Tahazadeh S, Mohammadi T, Tofighy MA, Khanlari S, Karimi H, Emrooz HBM (2021) Development of cellulose acetate/metal-organic framework derived porous carbon adsorptive membrane for dye removal applications. J Membr Sci 638:119692
Tam KH, Djurišić AB, Chan CMN, Xi YY, Tse CW, Leung YH, Chan WK, Leung FCC, Au DWT (2008) Antibacterial activity of ZnO nanorods prepared by a hydrothermal method. Thin Solid Films 516(18):6167–6174
Tang E, Cheng G, Ma X (2006) Preparation of nano-ZnO/PMMA composite particles via grafting of the copolymer onto the surface of zinc oxide nanoparticles. Powder Technol 161(3):209–214
Tanvidkar P, Nayak B, Kuncharam BVR (2023) Study of dual filler mixed matrix membranes with acid-functionalized MWCNTs and metal-organic framework (UiO-66-NH2) in cellulose acetate for CO_2 separation. J Polym Environ 31(8):3404–3417
Tien C (1994) Adsorption calculations and modelling. Elsevier, New York
Tye YY, Lee KT, Abdullah WNW, Leh CP (2011) Second-generation bioethanol as a sustainable energy source in malaysia transportation sector: status, potential and future prospects. Renew Sustain Energy Rev 15(9):4521–4536
United States Department of Agriculture (2024) Palm Oil Explorer. https://ipad.fas.usda.gov/cropexplorer/cropview/commodityView.aspx?cropid=4243000&sel_year=2024&rankby=Production
van den Berg O, Capadona JR, Weder C (2007) Preparation of homogeneous dispersions of tunicate cellulose whiskers in organic solvents. Biomacromol 8(4):1353–1357
Vasanth D, Prasad AD (2019) Ceramic membrane: synthesis and application for wastewater treatment—a review. Water resources and environmental engineering II. Springer, Singapore, pp 101–116
Vatanpour V, Pasaoglu ME, Barzegar H, Teber OO, Kaya R, Bastug M, Khataee A, Koyuncu I (2022) Cellulose acetate in fabrication of polymeric membranes: a review. Chemosphere 295:133914
Wahid MB, Abdullah SNA, Henson IE (2005) Oil palm — achievements and potential. Plant Prod Sci 8(3):288–297
Wang Z, Liu G, Fan Z, Yang X, Wang J, Wang S (2007) Experimental study on treatment of electroplating wastewater by nanofiltration. J Membr Sci 305(1–2):185–195
Wang Z-P, Xue M, Huang K, Liu Z (2011) Textile dyeing wastewater treatment. Intechopen, Croatia
Wei DW, Wei H, Gauthier AC, Song J, Jin Y, Xiao H (2020) Superhydrophobic modification of cellulose and cotton textiles: methodologies and applications. J Bioresour Bioprod 5(1):1–15
Wells RFD (1976) Structural inorganic chemistry. Clarendon Press, Oxford
Wibowo AC, Misra M, Park H-M, Drzal LT, Schalek R, Mohanty AK (2006) Biodegradable nanocomposites from cellulose acetate: mechanical, morphological, and thermal properties. Composites Part A 37(9):1428–33
Wu J, Xue D (2011) Progress of science and technology of ZnO as advanced material. Sci Technol Adv Mater 3(2):127–149
Yang B, Zhang M, Zhaoqing Lu, Tan J, Luo J, Song S, Ding X, Wang L, Peng Lu, Zhang Q (2019) Comparative study of aramid nanofiber (ANF) and cellulose nanofiber (CNF). Carbohyd Polym 208:372–381
Yang Z, Zhou Y, Feng Z, Rui X, Zhang T, Zhang Z (2019) A review on reverse osmosis and nanofiltration membranes for water purification. Polymers 11(8):1252. https://doi.org/10.3390/polym11081252
Yang M, Lotfikatouli S, Chen Y, Li T, Ma H, Mao X, Hsiao BS (2022) Nanostructured all-cellulose membranes for efficient ultrafiltration of wastewater. J Membr Sci 650:120422
Yusoff S (2006) Renewable energy from palm oil – innovation on effective utilization of waste. J Clean Prod 14(1):87–93
Zakaria N, Rohani R, Mohtar WHMW, Purwadi R, Sumampouw GA, Indarto A (2023) Batik effluent treatment and decolorization—a review. Water 15(7):1339
Zavastin D, Cretescu I, Bezdadea M, Bourceanu M, Drăgan M, Lisa G, Mangalagiu I, Vasić V, Savić J (2010) Preparation, characterization and applicability of cellulose acetate–polyurethane blend membrane in separation techniques. Colloids Surf A 370(1):120–28
Zhang W, Yang Y, Ziemann E, Beer A, Bashouti MY, Elimelech M, Bernstein R (2019) One-step sonochemical synthesis of a reduced graphene oxide – ZnO nanocomposite with antibacterial and antibiofouling properties. Environ Sci Nano 6(10):3080–3090
Zhao J, Zhang W, Zhang X, Zhang X, Canhui Lu, Deng Y (2013) Extraction of cellulose nanofibrils from dry softwood pulp using high shear homogenization. Carbohyd Polym 97(2):695–702
Zhou D, Zhang L, Zhou J, Guo S (2004) Cellulose/chitin beads for adsorption of heavy metals in aqueous solution. Water Res 38(11):2643–2650
Zhou J, Chen J, He M, Yao J (2016) Cellulose acetate ultrafiltration membranes reinforced by cellulose nanocrystals: preparation and characterization. J Appl Polym Sci. https://doi.org/10.1002/app.43946
Zhou D, Kang Z, Liu X, Yan W, Cai H, Jiaqiang X, Zhang D (2023) High sensitivity ammonia QCM sensor based on ZnO nanoflower assisted cellulose acetate-polyaniline composite nanofibers. Sens Actuators B Chem 392:134072
Zugenmaier P (2004) 4. Characteristics of cellulose acetates 4.1 characterization and physical properties of cellulose acetates. Macromol Symp 208(1):81–166
Zuo H-R, Shi P, Duan M (2020) A review on thermally stable membranes for water treatment: material, fabrication, and application. Sep Purif Technol 236:116223

Publisher's Note

Springer Nature remains neutral with regard to jurisdictional claims in published maps and institutional affiliations.